

# The tryptophan aminotransferase Tam1 catalyses the single biosynthetic step for tryptophan-dependent pigment synthesis in *Ustilago maydis*

Katja Zuther,<sup>1</sup> Peter Mayser,<sup>2</sup> Ursula Hettwer,<sup>3</sup> Wenying Wu,<sup>1†</sup> Peter Spiteller,<sup>4</sup> Bernhard L. J. Kindler,<sup>4</sup> Petr Karlovsky,<sup>2</sup> Christoph W. Basse<sup>1</sup> and Jan Schirawski<sup>1\*</sup>

<sup>1</sup>Max-Planck-Institute for Terrestrial Microbiology, 35043 Marburg, Germany.

<sup>2</sup>Center for Dermatology and Andrology, Justus Liebig University, 35385 Gießen, Germany.

<sup>3</sup>University of Göttingen, Department of Crop Sciences, 37077 Göttingen, Germany.

<sup>4</sup>Technische Universität München, Institute for Organic Chemistry and Biochemistry II, 85747 Garching, Germany.

## Summary

Tryptophan is a precursor for many biologically active secondary metabolites. We have investigated the origin of indole pigments first described in the pityriasis versicolor-associated fungus *Malassezia furfur*. Some of the identified indole pigments have properties potentially explaining characteristics of the disease. As *M. furfur* is not amenable to genetic manipulation, we used *Ustilago maydis* to investigate the pathway leading to pigment production from tryptophan. We show by high-performance liquid chromatography, mass spectrometry and nuclear magnetic resonance analysis that the compounds produced by *U. maydis* include those putatively involved in the etiology of pityriasis versicolor. Using a reverse genetics approach, we demonstrate that the tryptophan aminotransferase Tam1 catalyses pigment biosynthesis by conversion of tryptophan into indolepyruvate. A forward genetics approach led to the identification of mutants incapable of producing the pigments. These mutants were affected in the *sir1* gene, presumably encoding a sulphite reductase. *In vitro* experiments with purified Tam1 showed

that 2-oxo 4-methylthio butanoate serves as a substrate linking tryptophan deamination to sulphur metabolism. We provide the first direct evidence that these indole pigments form spontaneously from indolepyruvate and tryptophan without any enzymatic activity. This suggests that compounds with a proposed function in *M. furfur*-associated disease consist of indolepyruvate-derived spontaneously generated metabolic by-products.

## Introduction

The amino acid tryptophan (Trp) serves as a precursor for many secondary metabolites with diverse biological effects. Prominent Trp derivatives include the ergot alkaloids of fungi [e.g. the mycotoxin ergotamine produced by *Claviceps purpurea* (Tudzynski *et al.*, 1999)], the antibiotic dye violacein from *Chromobacterium violaceum* (Balibar and Walsh, 2006), the anti-tumourigenic indole-carbazoles staurosporine and rebeccamycin produced by various actinomycetes (Sanchez *et al.*, 2006), the plant growth hormone indole acetic acid (IAA) (Vogler and Kuhlemeier, 2003), the phytoalexins produced by plants in response to pathogen attack (Pedras *et al.*, 2000), the ommochromes determining insect eye colour (Oxford and Gillespie, 1998) and industrially relevant pigments such as indigo (Russell and Kaupp, 1969). Recently, a whole new set of Trp-derived compounds with a proposed function in the *Malassezia*-associated skin disease pityriasis versicolor was isolated from the basidiomycetous yeast *Malassezia furfur* (Mayser *et al.*, 2003; Irlinger *et al.*, 2004; Krämer *et al.*, 2005a; Machowinski *et al.*, 2006).

*Malassezia furfur* occurs naturally on human skin and has been implicated in the disease pityriasis versicolor. The disease is characterized by scaly hyperpigmented or hypopigmented lesions that show only minor signs of inflammation (Charles *et al.*, 1973; Gupta *et al.*, 2003). These lesions display a characteristic yellow-greenish fluorescence that can be used for diagnosis (Thoma *et al.*, 2005). While the fungal infection itself can efficiently be treated with anti-mycotic drugs, the associated hypopigmentation of the affected skin areas usually persists for several months (Thoma *et al.*, 2005). Interestingly,

Accepted 24 January, 2008. \*For correspondence. Email schiraws@mpi-marburg.mpg.de; Tel. (+49) 6421 178601; Fax (+49) 6421 178609. †Present address: Smithsonian Institution, Department of Paleobiology, MRC 121, Washington DC 20013, USA.

hypopigmented skin areas do not show an increased sensitivity to UV-irradiation (Larangeira de Almeida and Mayser, 2006). In addition, these lesions seem to contain a lower amount of melanin, which has been correlated to a reduced size and aggregation of melanosomes as well as to the plasmolysis of melanocytes (Galadari *et al.*, 1992).

*Malassezia furfur* produces a large variety of fluorescent and coloured compounds (pigments) from Trp (Mayser *et al.*, 1998), and some of these have been purified and their chemical structure determined (Mayser *et al.*, 2002; 2003; Irlinger *et al.*, 2005; Krämer *et al.*, 2005a; Machowinski *et al.*, 2006). These novel compounds display biological effects that can explain specific disease characteristics. Pityriarubrine (PyA; Fig. 1A) and the pityriarubins A, B and C (PitA, PitB, PitC; Fig. 1A) can act *in vivo* as anti-inflammatory agents, thus potentially explaining the modest levels of inflammation observed in affected skin areas (Krämer *et al.*, 2005b). Pityriacitrin (PCit; Fig. 1A) has been described as a highly potent UV-filter (Mayser *et al.*, 2002; Machowinski *et al.*, 2006) that could explain why depigmented skin areas are protected from sunburn. Malassezin, a novel type of aryl hydrocarbon receptor (AhR) agonist, induces apoptosis in human melanocytes and could thus contribute to the development of the characteristic depigmented skin lesions (Krämer *et al.*, 2005a). Finally, the compound pityrialactone is a fluorochrome and could contribute to the fluorescence used for diagnosis (Mayser *et al.*, 2003). Very recently, Trp-derived pigments with an identical structure to those of *M. furfur* have been found in extracts of *Candida glabrata* grown on Trp agar, possibly indicating evolutionary conservation of biosynthetic pathways (Mayser *et al.*, 2007).

The biosynthetic pathways for the generation of some secondary metabolites derived from Trp have been completely or partially resolved. The first specific enzyme of the ergotamine biosynthesis pathway of *C. purpurea* (Tudzynski *et al.* 2001) is dimethylallyltryptophan (DMAT) synthase, which catalyses the formation of DMAT from Trp and dimethylallylpyrophosphate (Tsai *et al.*, 1995). The five biosynthetic enzymes for generation of the anti-tumourigenic bis-indolyl quinone terrequinone A of *Aspergillus nidulans* are encoded on a gene cluster. The first step consists of deamination of Trp to indole pyruvic

acid (IPA) catalysed by TdiD, followed by IPA dimerization catalysed by the non-ribosomal peptide synthetase module TdiA (Balibar *et al.*, 2007; Schneider *et al.*, 2007). The biosynthesis of violacein, a water-insoluble purple pigment produced by *C. violaceum*, begins with the oxidative dimerization of two molecules of Trp catalysed by the Trp oxidase VioA and a heme-containing oxidase VioB (Balibar and Walsh, 2006). Very similar reactions are involved in the biosynthesis of the indolocarbazoles staurosporine and rebeccamycin, substances with anti-tumourigenic effects produced by different actinomycetes (Sanchez *et al.*, 2006).

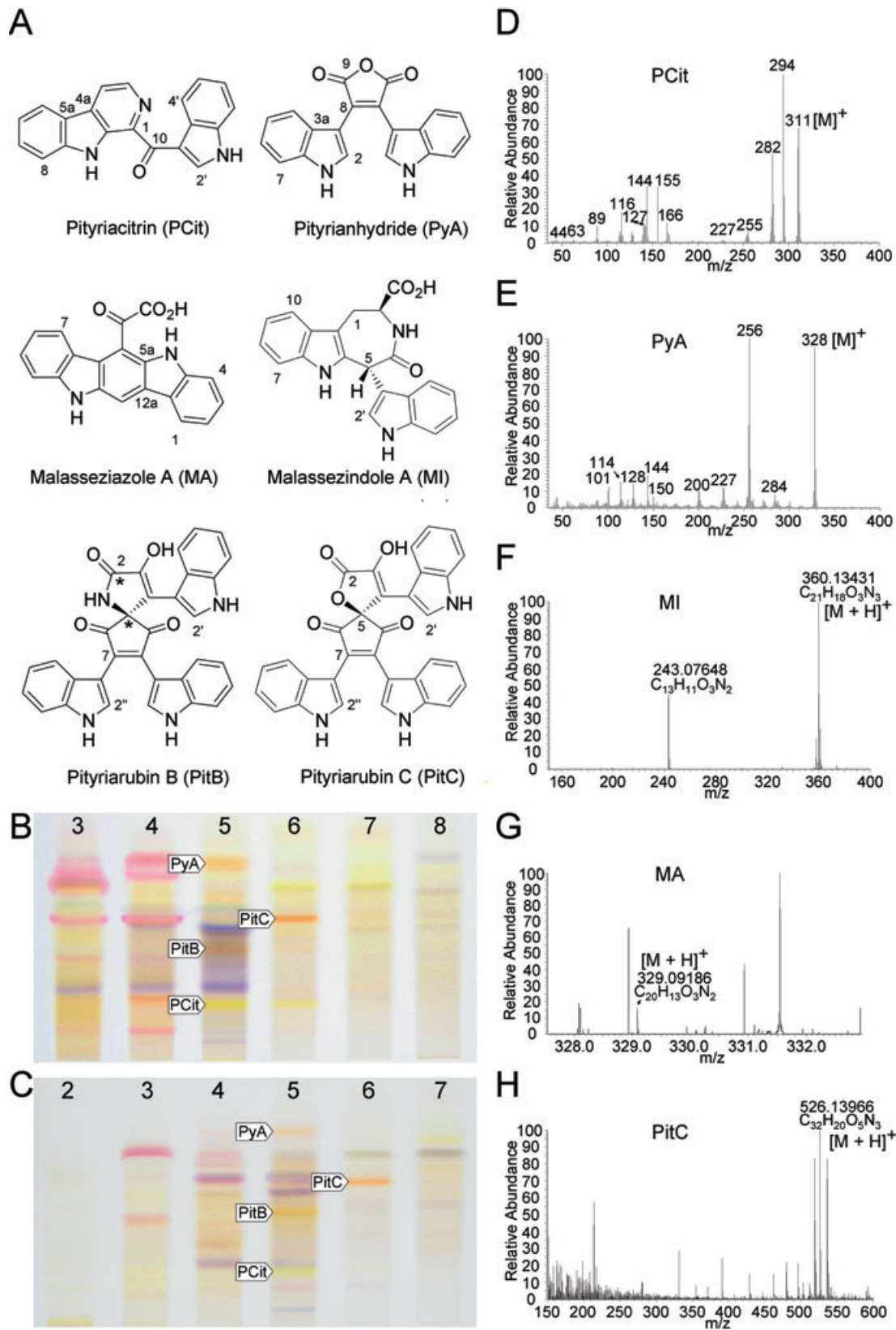
Several pathways exist for the Trp-dependent synthesis of IAA (Teale *et al.*, 2006), a plant growth hormone, which also functions as a virulence factor and signalling molecule in diverse bacterial species (Spaepen *et al.*, 2007). In plants, Trp can either be decarboxylated to tryptamin, which might then be converted to indole acetaldoxime (IAOx), or can be directly converted to IAOx using a cytochrome P450 enzyme. IAOx represents a potential precursor of IAA either via the intermediate indole-3-acetonitrile, or via indole acetaldehyde (IAAld). In an independent pathway, Trp can be deaminated to indolepyruvate (IP), which is then oxidized via IAAld to IAA (see reviews by Ljung *et al.*, 2002; Woodward and Bartel, 2005). Fungi have also been reported to produce IAA (Gruen, 1959); however, the biosynthetic mechanisms have not been elucidated. As the plant pathogenic fungus *Ustilago maydis* induces tumours on its host plant maize, IAA has been proposed to be involved in symptom formation (Wolf, 1952).

For the biosynthesis of the novel compounds identified from *M. furfur*, a triketone precursor, 4,5-bis-(1*H*-indol-3-yl)-cyclopent-4-ene-1,2,3-trione, was proposed that could be formed by condensation of two molecules of IP (Irlinger *et al.*, 2004). This precursor was proposed to either react with Trp to yield PitA or with indolylpyruvamide or the corresponding carboxylic acid to yield PitB and PitC respectively (Irlinger *et al.*, 2004). For biosynthesis of PyA and pityrialactone from the proposed triketone intermediate, a number of oxidation and decarboxylation reactions were predicted (Irlinger *et al.*, 2004). [ $1'$ - $^{13}\text{C}$ ]Trp feeding experiments revealed that the spiro carbon atoms of the pityriarubins (marked by an asterisk in PitB, Fig. 1A) stem from the carboxy group of Trp, whereas the carboxy group

**Fig. 1.** Compounds produced by both *M. furfur* and *U. maydis*.

A. Chemical structure of compounds identified in pigment extracts of Trp plates inoculated either with *U. maydis* or with *M. furfur*. The asterisks in the structure of PitB mark the spiro carbon atoms that were labelled in [ $1'$ - $^{13}\text{C}$ ]Trp feeding experiments of *M. furfur* (Irlinger *et al.*, 2004).

B and C. TLC profiles of consecutive fractions eluting from a Sephadex LH-20 column from pigment extracts of *M. furfur* (B) and *U. maydis* (C) grown on Trp agar. Open arrows mark compounds with proposed biological effects (from top to bottom): PyA, PitC, PitB, PCit. D–H. Mass spectra from purified compounds isolated from *U. maydis*-inoculated Trp agar. Shown are EI-MS spectra (70 eV) of PCit (D) and PyA (E), and HR-ESI-MS spectra of MI (F), MA (G) and PitC (H).



of the second Trp is lost, suggesting a decarboxylation reaction (Irlinger *et al.*, 2004).

Investigation of biosynthetic pathways and study of the role of Trp-derived pigments in the pathogenesis of *M. furfur* is hampered by the lack of vectors and an available transformation system for *M. furfur*. To overcome these constraints, we sought to investigate the capacity of other organisms to produce pigments from Trp. We have chosen *U. maydis*, a plant pathogenic fungus causing maize smut disease, as the most closely related organism whose genome has been sequenced (Kämper *et al.*, 2006) and where genetic manipulation is well established (Bölker *et al.*, 1995). Here we report the isolation of indolic pigments from cultures of *U. maydis* that are identical to those produced by *M. furfur*, thus proving the suitability of *U. maydis* as a model organism for the study of the biosynthetic pathways of these novel compounds. Using *U. maydis*, we were able to demonstrate that the first biosynthetic step for the generation of the novel indole compounds is catalysed by the Trp aminotransferase Tam1 that converts Trp into IP. We show that these indole pigments with demonstrated biological effects are generated from IP alone or IP and Trp through spontaneous chemical reactions, which do not involve enzymatic activities. Thus, only one biosynthetic step is required to produce a multitude of structurally complex compounds from Trp.

## Results

### *Parallels in Trp-dependent indole pigment production of M. furfur and U. maydis*

Preliminary experiments indicated that *U. maydis* is capable of generating brownish pigments when grown in the presence of Trp under conditions previously established for pigment production of *M. furfur*. To identify the nature of the produced compounds, pigments were extracted with ethyl acetate (EtOAc) from plates inoculated either with *U. maydis* or *M. furfur*. Pigment extracts were further purified by column chromatography on Sephadex LH-20, and different fractions were collected. Thin-layer chromatography (TLC) on silica gel plates of these fractions revealed that both fungi produce a great number of differently coloured compounds (Fig. 1B and C). In addition, multiple compounds seemed to occur in both pigment extracts of both organisms (Fig. 1B and C). Neither of the two fungi produced any visible pigments when Trp was replaced by arginine in the growth medium (not shown).

To elucidate the identity of the compounds produced by *U. maydis*, selected pigments were isolated from preparative silica gel TLC plates and purified by high-performance liquid chromatography (HPLC) on an RP-8 phase. Indi-

vidual compounds were analysed by nuclear magnetic resonance (NMR) spectroscopy and liquid chromatography high resolution electrospray ionization mass spectrometry (LC-HR-ESI-MS) or electron impact mass spectrometry (EI-MS). By comparison of the obtained spectroscopic data with published data (Brenner *et al.*, 1988; Mayser *et al.*, 2002; Irlinger *et al.*, 2004; 2005), the identity of the compounds PCit, PyA, malassezindole A (MI) and malasseziazole A (MA) were unequivocally identified (Fig. 1D–G and *Experimental procedures*). The presence of PitC in *U. maydis* extracts was proven by comparison of its LC-ESI-MS with the corresponding LC-ESI-MS of an authentic sample of PitC (Fig. 1H and *Experimental procedures*). Thus, *U. maydis* is obviously able to synthesize compounds identical to those produced by *M. furfur*. This confirms the suitability of *U. maydis* as a model organism for the elucidation of the biosynthetic pathway of Trp-derived indole pigments.

### *Identification of pigment-deficient mutants in U. maydis*

To identify genes involved in pigment biosynthesis, *U. maydis* wild-type strain 521 was subjected to UV mutagenesis and subsequently screened for loss of dark-brown colony colour on agar plates containing Trp (see *Experimental procedures*). In two different mutagenesis experiments,  $3 \times 10^7$  cells each were plated on Trp agar plates and UV-irradiated to a survival rate of 1%. In this way, we generated in total approximately  $10^5$  mutants, of which 44 were different in colour from the wild type. Of all generated mutants, only five (UV31 of the first mutagenesis experiment, WW01, WW02, WW03 and WW04 of the second mutagenesis experiment) displayed a complete pigment production deficiency on Trp agar. The small number of identified mutants might suggest the involvement of very few genes for pigment biosynthesis, or the existence of multiple parallel biosynthetic pathways.

The five identified non-coloured mutants grew well on complete media but showed a severe growth defect on agar containing Trp as sole nitrogen source (Fig. 2A). To identify the affected genes, one of the mutants, UV31, was transformed with a genomic library of *U. maydis* on an autonomously replicating plasmid that confers resistance to hygromycin. Plasmids conferring restored pigment production capabilities were re-isolated from transformants with brown colony colour, amplified in *Escherichia coli* and end-sequenced. Resulting sequences were compared with the genome sequence of *U. maydis* (MUMDB; <http://mips.gsf.de/genre/proj/ustilago/>). Inserts of complementing plasmids contained different fragments of the *U. maydis* genome that overlapped in one region (Fig. 2D, upper part). This region contained a single open reading frame (ORF; um02922) showing 43% amino acid identity to Ecm17p from *S.*

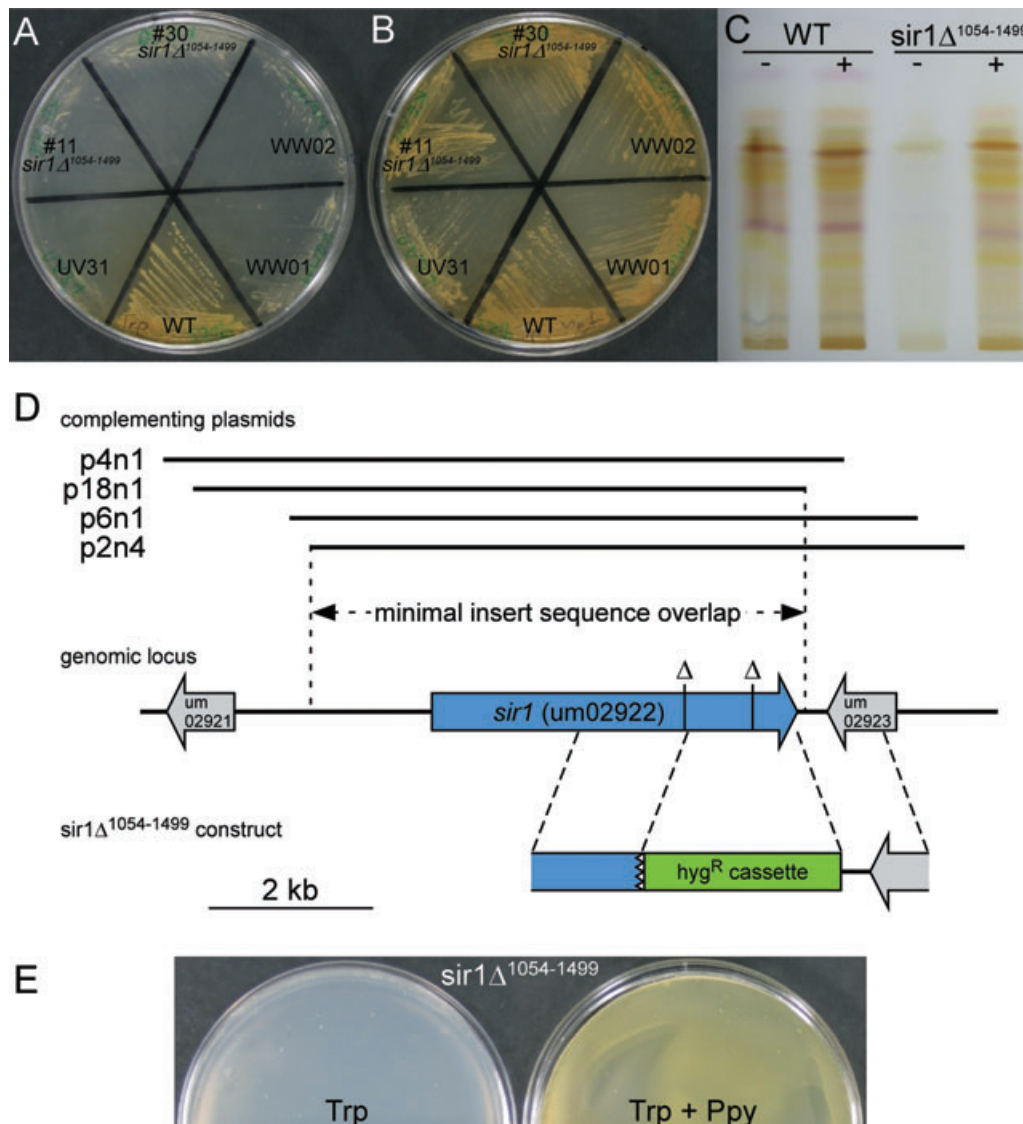


**Fig. 2.** Identification of *sir1* as a gene involved in sulphur metabolism and pigment biosynthesis.

A. Mutants generated by UV mutagenesis (UV31, WW01 and WW02), as well as mutants carrying a C-terminal deletion of the *sir1* ORF (*sir1* $\Delta^{1054-1499}$ , strains #30 and #11) show a growth defect as well as a pigmentation defect on Trp agar after growth for 2 days at 28°C.

B. The pigmentation-deficient phenotype can be rescued by addition of Met. Strains (as in A) were streaked on Trp agar containing Met and grown for 2 days at 28°C.

C. Comparison of non-fractionated pigment profiles by TLC of strains 521 (WT) and 521*sir1* $\Delta^{1054-1499}$ #30 (*sir1* $\Delta^{1054-1499}$ ) grown on Trp agar without (-) or with (+) the addition of Met.

D. Identification of mutations present in pigmentation-deficient UV-generated mutants. Mutant UV31 was complemented with a genomic library of *U. maydis*. Black horizontal lines (top) indicate insert sequences from complementing plasmids p4n1, p18n1, p6n1 and p2n4 compared with the relevant fraction of the genome of *U. maydis* (middle) (MUMDB, <http://mips.gsf.de/genre/proj/ustilago/>). The minimal insert sequence overlap contains only the *sir1* gene.  $\Delta$  symbols indicate the position of 1 bp deletions present in the *sir1* ORF (blue arrow) of UV31, WW01, WW03 and WW02, predicted to lead to C-terminally truncated Sir1 proteins. Below is depicted the construct for replacement of the C-terminal part of *sir1* with a hygromycin-resistance cassette (*hyg*<sup>R</sup>, green rectangle).

E. The pigment production defect of the 521*sir1* $\Delta^{1054-1499}$ #11 strain can be complemented by the addition of PPy. An overnight culture of 521*sir1* $\Delta^{1054-1499}$ #11 was thoroughly washed with water (see *Experimental procedures*), and plated on Trp agar without (left) or with (right) 1 mM PPy.

*cerevisiae*. Ecm17p encodes a sulphite reductase beta subunit (Kobayashi and Yoshimoto, 1982). Based on their high sequence identity and additional experimental evidence (see below), um02922 of *U. maydis* potentially

encodes a nitrite/sulphite reductase and was therefore named *sir1* (Fig. 2D, middle part).

One of these plasmids (p18n1) was tested for complementation activity by introduction into four of the five

pigment deficient mutants (UV31, WW02, WW03 and WW04). Surprisingly, all transformed mutants regained pigment production capabilities upon introduction of p18n1, indicating that the same gene was affected in all four identified UV-generated strains (not shown).

To verify whether the absence of a functional sulphite reductase was responsible for the loss of pigment production on Trp agar plates, we tried to delete the complete *sir1* ORF. However, numerous attempts to generate a deletion mutant failed, suggesting that the gene is essential. To analyse mutations in the *sir1* gene or its promoter regions, the corresponding sequences from four of the five mutants (UV31, WW01, WW02 and WW03) were amplified and compared with the wild-type sequence. This showed that in mutants UV31, WW01 and WW03, a single base pair deletion had taken place (nt 3113 of the *sir1* ORF) that would lead to a frame shift and a protein lacking the C-terminal domain. While WW01 and WW03 were generated in the same mutagenesis experiment and could potentially be siblings, UV31 is an independently generated mutant. For mutant WW02, another single base pair deletion was detected (nt 3947 of the *sir1* ORF), which would also lead to a frame shift and a protein lacking the C-terminal domain (Fig. 2D, middle part).

To verify that the lack of the C-terminal domain of Sir1 was responsible for the loss of pigment production, we generated mutants 521sir1 $\Delta^{1054-1499}$ #11 and 521sir1 $\Delta^{1054-1499}$ #30 carrying a deletion of the C-terminal domain only (amino acids 1054–1499; sir1 $\Delta^{1054-1499}$ ; Fig. 2D, lower part). Both mutants displayed a pigmentation loss as well as a growth defect on Trp plates comparable to the UV-generated mutants (Fig. 2A), corroborating that the observed phenotype was due to a non-functional Sir1 C-terminal domain.

As Sir1 potentially encodes a sulphite reductase, we tested whether the observed phenotypes could be complemented by exogenous addition of reduced sulphur to agar plates. Both pigment production and growth on Trp could be restored by the addition of methionine (Met), cysteine or sodium sulphide to the agar plates but not by addition of sodium sulphate or sodium sulphite (Fig. 2B and not shown), suggesting that *sir1* may encode a sulphite reductase.

To find out whether the pigment profile of the sir1 $\Delta^{1054-1499}$  mutants was altered or whether pigment production was completely impaired, we extracted pigments from wild-type strain 521 or mutant 521sir1 $\Delta^{1054-1499}$ #30 grown on Trp plates in the absence or presence of Met. TLC of total extracts revealed that mutant 521sir1 $\Delta^{1054-1499}$ #30 produced fewer pigments and showed an overall dramatic reduction in pigment synthesis. However, presence of Met in the growth medium restored the pigment pattern (Fig. 2C). The inability of the identified mutants to produce either pigments or Met suggested a link between pigment formation and Met biosynthesis (see *Discussion*). Prompted by this finding, we followed a reverse genetics approach for the identification of additional genes involved in pigment biosynthesis.

#### Identification of a pigment biosynthetic gene using a reverse genetics approach

Based on the chemical structure of the isolated compounds, we postulated the deamination of Trp to be an essential step during pigment biosynthesis. In *Saccharomyces cerevisiae*, two enzymes, Aro8 and Aro9, catalyse the deamination of Trp. To identify genes potentially encoding Trp transaminases in *U. maydis*, we performed a BLAST search using Aro8 and Aro9 as query sequences (Altschul *et al.*, 1990). This indicated the possible presence of two tryptophan transaminases [*tam1* (um01804, MUMDB, <http://mips.gsf.de/genre/proj/ustilago/>) and *tam2* (um03538, MUMDB, <http://mips.gsf.de/genre/proj/ustilago/>)] in the genome of *U. maydis*. Both genes showed equal amino acid identity of 26% to Aro8 and about 20% to Aro9 (ClustalW, Larkin *et al.*, 2007) and showed conservation of the residues involved in pyridoxal-phosphate binding (see Fig. 3A).

To investigate whether one or both of these genes play a role in pigment biosynthesis, we generated derivatives of *U. maydis* wild-type strain 521 carrying either single deletions of *tam1* or *tam2*, or deletions of both genes (Table 1). These strains were tested for their capacity to produce pigments on Trp agar. Trp plates incubated with wild type and 521 $\Delta$ tam2 showed a darker colour than those incubated with 521 $\Delta$ tam1 or 521 $\Delta$ tam1 $\Delta$ tam2

**Fig. 3.** Tam1 of *U. maydis* is involved in Trp-dependent pigment production.

- A. Alignment of the amino acid sequences of Tam1 and Tam2 of *U. maydis*, and Aro8 and Aro9 of *S. cerevisiae*. Green stars mark amino acids predicted to be involved in direct binding of pyridoxal-phosphate by comparison with other aminotransferases (Sung *et al.*, 1991). Conserved amino acids are highlighted in red (conserved in all four protein sequences) or blue (conserved in three of the four protein sequences).
- B. Strains 521 $\Delta$ tam1 ( $\Delta$ tam1) and 521 $\Delta$ tam1 $\Delta$ tam2 ( $\Delta$ tam1 $\Delta$ tam2) show less pigment production than the wild-type strain 521 (WT) or 521 $\Delta$ tam2 ( $\Delta$ tam2) after growth on Trp agar for 3 days at 28°C.
- C. Comparison of fractionated pigment profiles by TLC of strains shown in B grown on Trp agar.
- D. Presence of selected compounds in the fractions shown in C was analysed by LC-ESI-MS (PitC, PitB) or MS/MS (PyA, PCit). Trace amounts and not detected represent signal to noise ratios below 30 and below 10 respectively.

A

```

Tam1  MTPSAQVANVDPNPYFGDKVGLASTSETYPKASRVDPARFLSQVSHDMPASAIRS---LPPAELIPGMLSILAKKQNPDTFFESLSLN-----LKPEA--E-AG   95
Tam2  MSSATSPA-----LDYALLSSARNMPSAIRS---LPPAELIPGMLSILSKQNSETFQFQRIISLE-----LKPSIHLE-GQ   70
Aro8  MTLPESEK-----DPSYLFSEDTNAKPSPLKTCIHLFQD---FNIIIFGGGLPLKDYFFWDLNLSVDSKPPFPQGGIAPIDEQNCIKYTVNKDYAD   88
Aro9  MTAGSAP---PVVDY-----TSLKKNQFPFLRRVENSLKSFWD---ASDISDDVIELAGKQNERFFIEISMDLKIISKVPFNDNP---KWHNSFT-THALDLS   90

Tam1  PTQLNIQGEDLVSALOYGATSIIRKIVQNIITELQVHMEREAVTPGSKLDGVAGRTPNRVITGNSSQDLLNKTFDALLNPGDVIIVLSPAYTGIIPSLVMIKANIVFVTS----DDQG   209
Tam2  TETVSIEGSDLDIALQYSATSRLPKQVDWIIKQSRVHARKQVDEGNKPGEV---WRCDFGNSQDLLKTFEALVDAGDSVVLSPAYSGLIPSLVAHKANLFEAET----DAEG   179
Aro8  KSANPSNDIPLSRALQYGFSAQPEELNFIIRDHTKIIHDLKYKD-----NDVLATANTNAWESTLRVFCNRGDVILVAHSFSSSLASAEAGQVITFFVPI----DADG   189
Aro9  PSELPI----ARSFQAEATKLEPLLHFVKDFVSRINRPAFSDETE-----SNDDVILSGGNSDMFKVFETICESTVMIEEFTTTPAMSNVEATGAKVPIPKNLTFDRESQ   197

Tam1  MMSRLAEILANRETDPQASLARPKCLYITPTGANPASTTASDERKRRQILALARQYDFVLEDDPTYYH---FEGLDQ--DAVTRPR-----CRSYWSIEEHRERWGTGR   312
Tam2  VEPTALDTLLTNKTDASATRSRFFKFLYITPTGANPSTTSASDNKRRAILDIIIRKHNLLLEDDPTYYLS---FQGLEPGADAVKRRR-----GKSYFOLEAQ--DDYGVGR   282
Aro8  IIEPKLAKVMEN---TPGAPKRLLYTIPTGNETTSTIADHRKEATYKIAQKYDFLIVEDEPTYFLQMNPIKDLKEREKQSSPKQDHFELKS-LANTFLSLDTE---GR   296
Aro9  IDVEYITQLLDNMSIGPY-KDLNKRVLTYIATGNETMMSVPOWKREKTYQLAQRHDFLIVEDDPYGYLYFPSY-NPQEPLENPYHSSDLTTERYLNDFLMKSEFLTIDTD-----AR   308

Tam1  VIFESFSKILAAELRIGFATGPNEIDAVDANTAMSNLQPSLAGVVAYTLLNYNGIP-----FLRHVDNVARYAKRRDNFEAKANKVL-GAAGVAQVVTIVKSMELW   416
Tam2  VVFDPSFKILSACLRLGFVTGPKEIDDAIDLTSSRNLTSTTSQAIAYALLSKNGID-----GFLHADVARYQNRLEFEASAQAILTGSPSIASWVRVSAQSMELW   387
Aro8  VIFMDSFSKVLAPSTRLQWITGSSKIKPFLSLHEMTIQAPAGFTQVLVNAITLSRWGQK-----GYLDWLLGLRHEYTLKRDCAIDALYKYLQSDAFVI-NPPIAGMFT   400
Aro9  VIFLETFSKIFAPSLRISFIVANKFLQKILDLADITTRAPSTSQAIVYSTIKAMAENLSSSLSMKEAMFEWIRWIMQIASKYNHRKNTLKLALYETESYQAGQFTVMEISAGMFTII   427

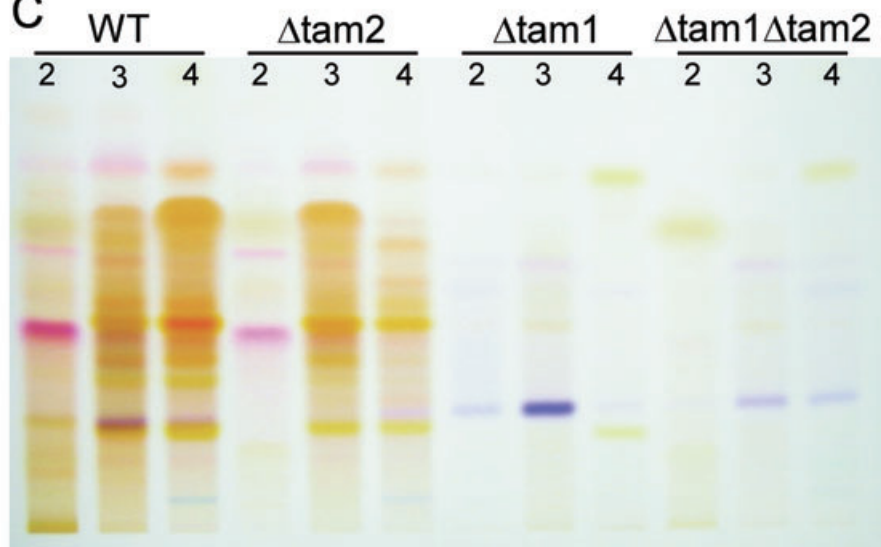
Tam1  LRLN---LPPTQGESEGSFAL---ISDKAKAAGVLAIVGVAFI-----PDGSKSC-----YVTSFS-IIAEDDVEEAFNLRNVVLDADWDAGKMPPELA   503
Tam2  IKLK---LPPSPDS-AEGDSFDL---ISNKAKAAGVLAIVGVAFK-----PSSSSTGGKRRKTSAYVTSFS-QVPLDQVDATFLRQVVVEAWREAGLQIPA   479
Aro8  VNID-ASVHPEFKTKYNSDYQLQSLYKVVVERGVVVPGSWFKSEGETEPPQPAESKEVSNPNIIFFGTYA-AVSPEKLTGLKGLDGLTYEEFGI-SK   500
Aro9  IKINWGNFD---RPDDLQPMQILDKFLILNGVKVVLG-----YKM-----AVCPNYSKQNSDFLELTIAIYARDDQLIEASKIGSGIKEFPDN-YKS   513

```

B



C



D

	WT	$\Delta tam2$	$\Delta tam1$	$\Delta tam1\Delta tam2$
PyA	+	+	+	+
PitC	+	+	nd	nd
PitB	a	nd	nd	nd
PCit	+	+	+	+

a, trace amounts; nd, not detected

**Table 1.** *U. maydis* strains used in this study.

Strain	Transformant	Genotype	Progenitor strain	Deletion construct <sup>a</sup>	Resistance	Source or reference
521		<i>a1b1</i>				R. Holliday
521Δ <i>tam1</i>	#2	<i>a1b1 tam1</i> Δ	521	<i>tam1</i> Δ	cbx	This work
521Δ <i>tam2</i>	#2	<i>a1b1 tam2</i> Δ	521	<i>tam2</i> Δ <i>nat</i>	nat	This work
521Δ <i>tam1</i> Δ <i>tam2</i>	#4	<i>a1b1 tam1</i> Δ <i>tam2</i> Δ	521Δ <i>tam1</i>	<i>tam2</i> Δ	cbx, phleo	This work
521 <i>sir1</i> Δ <sup>1054–1499</sup>	#11, #30	<i>a1b1 sir1</i> Δ <sup>1054–1499</sup>	521	<i>sir1</i> Δ <sup>1054–1499</sup>	hyg	This work
SG200		<i>a1mfa2bE1bW2</i>			phleo	Bölker <i>et al.</i> (1995)
SG200Δ <i>tam1</i>	#2, #7	<i>a1mfa2bE1bW2 tam1</i> Δ	SG200	<i>tam1</i> Δ	phleo, cbx	This work

a. As described in *Experimental procedures*.

strains, indicating that 521Δ*tam1* strains are affected in pigment production from Trp (Fig. 3B). TLC of fractionated pigment extracts showed that 521Δ*tam2* was capable of producing the same pigment profile as the wild-type strain 521 (Fig. 3C). This indicates that *tam2* has at most a minor influence on pigment production. In contrast, the pigment profiles of 521Δ*tam1* and 521Δ*tam1*Δ*tam2* were different from that of the wild type. In both *tam1*Δ strains (521Δ*tam1* and 521Δ*tam1*Δ*tam2*), pigment production was severely affected, and they produced fewer compounds than the wild type (Fig. 3C). This shows that *tam1* plays a major role in the production of Trp-derived pigments in *U. maydis*.

Residual pigment production could be observed in extracts of *tam1*Δ strains, 521Δ*tam1* and 521Δ*tam1*Δ*tam2* (Fig. 3C). To investigate the identity of the remaining compounds, we analysed the extracts by LC-ESI-MS and MS/MS for the presence of PyA, PitC, PitB and PCit. This analysis revealed the presence of PyA and PCit in extracts of all four strains, 521, 521Δ*tam2*, 521Δ*tam1* and 521Δ*tam1*Δ*tam2* (Fig. 3D). While PitB was identified in trace amounts only in the wild-type extract and could not be detected in the extracts of the mutants, PitC was clearly present in the extracts of wild type and 521Δ*tam2* but could not be identified in extracts of *tam1*Δ strains (Fig. 3D). The presence of PyA and PitC in extracts of 521Δ*tam1* and 521Δ*tam1*Δ*tam2* could potentially be explained by the action of an additional enzyme with a weak activity for the conversion of Trp into IP. A likely candidate is the aspartate aminotransferase (potentially encoded by um00595, MUMDB, <http://mips.gsf.de/genre/proj/ustilago/>). Aspartate aminotransferases of other organisms have been shown to convert Trp into IP as a side reaction (Paris and Magasanik, 1981; Berger *et al.*, 2001; Bittinger *et al.*, 2003).

#### *Tam1 couples Trp deamination to the amination of phenylpyruvate*

Both Aro8 and Aro9 of *S. cerevisiae* catalyse the conversion of Trp into IP (Kradolfer *et al.*, 1982). To find out whether Tam1 also acts as a Trp transaminase that gen-

erates IP, we measured IP production of wild-type and *tam1*Δ mutants after Trp feeding. IP was extracted from supernatants of cultures grown in the presence of 5 mM Trp for 14 h, and measured as IPA by HPLC. *tam1*Δ mutants produced only very low amounts of IPA (4% of wild type), while *tam2*Δ mutants produced IP to wild-type levels (Fig. 4A). This suggests that Tam1 acts as a Trp aminotransferase that converts Trp into IP.

Aro8 and Aro9 of *S. cerevisiae* are known to transfer the amino group from Trp to 2-oxoglutarate (2-OG) and phenylpyruvate (PPy) respectively (Kradolfer *et al.*, 1982; Iraqui *et al.*, 1998; Urrestarazu *et al.*, 1998). To elucidate whether Tam1 uses 2-OG or PPy as amino acceptor, we investigated the effect of the addition of either 2-OG or PPy to the growth medium on the production of IPA from Trp. The addition of 1 mM PPy, but not 2-OG, to wild-type cells grown in the presence of 5 mM Trp led to an 18-fold increase in IPA production (Fig. 4B). In contrast, 521Δ*tam1* grown in the presence of Trp and PPy showed a 77% decrease in IPA production compared with the wild type grown under the same conditions. This indicates that Tam1 is active with PPy as amino acceptor, and thus couples the deamination of Trp to the amination of PPy, like Aro9 of *S. cerevisiae*. However, these experiments do not exclude the possibility that Tam1 can also use 2-OG as amino acceptor, as uptake of 2-OG might be inhibited in *U. maydis*.

Addition of PPy to the Δ*tam1* strain stimulated IPA production (Fig. 4B). This indicates the existence of additional enzymatic activities for PPy-dependent conversion of Trp into IP. Such activities might stem from Tam2 requiring higher levels of PPy for measurable activity, or from the potential aspartate aminotransferase (um00595, MUMDB, <http://mips.gsf.de/genre/proj/ustilago/>), as aspartate aminotransferases are known to have broad substrate specificities (Jensen and Gu, 1996).

The 521*sir1*Δ<sup>1054–1499</sup> strain is severely reduced in pigment production but carries a defect in the *sir1* gene, thus the *tam1* gene should be functional. To assess Tam1 activity in this background, we tested whether addition of PPy to the growth medium could restore pigment formation. Addition of PPy to the 521*sir1*Δ<sup>1054–1499</sup> strain

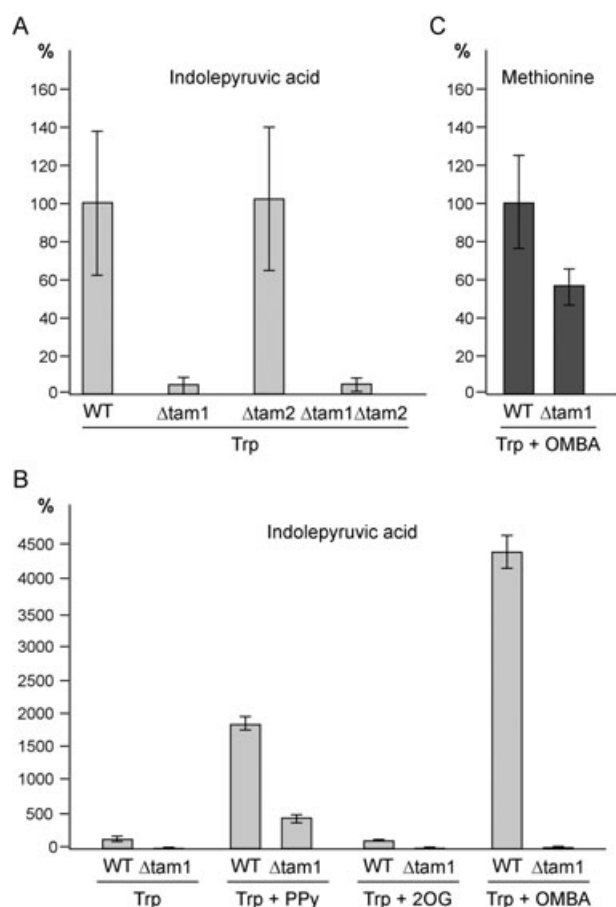


**Fig. 4.** Tam1 is involved in Trp to IP and OMBA to Met conversion.  
 A. Production of IPA of 521 (WT), 521 $\Delta tam1$  ( $\Delta tam1$ ), 521 $\Delta tam2$  ( $\Delta tam2$ ) and 521 $\Delta tam1 \Delta tam2$  ( $\Delta tam1 \Delta tam2$ ) after 14 h cultivation in CM containing glucose (1%) and Trp (5 mM). IPA levels are presented as percentage of wild-type average.  
 B. Production of IPA by wild-type (521, WT) and 521 $\Delta tam1$  ( $\Delta tam1$ ). Strains were grown in CM containing glucose (1%) and Trp (5 mM), and the addition of PPy (1 mM), 2-OG (1 mM) or OMBA (1 mM) as indicated. IPA levels are presented as percentage of wild-type average grown in CM containing glucose and Trp.  
 C. Production of Met by the strains used in B after growth in CM containing glucose (1%), Trp (5 mM) and OMBA (1 mM). Met levels are presented as percentage of wild-type average. Error bars indicate SEM of three replicate experiments.

stimulated pigment production (Fig. 2E). This shows that *sir1* is not directly involved in pigment formation. The reduced capacity of the 521 $sir1\Delta^{1054-1499}$  strain to produce pigments could be due to an insufficient level of suitable amino acceptors for the Tam1-catalysed conversion of Trp into IP. The level of amino acceptors seems to be dependent on the function of Sir1 (see *Discussion*).

#### *Tam1 couples Trp deamination to the amination of 2-oxo 4-methylthio butanoic acid*

In *S. cerevisiae*, Aro9 can also catalyse the amination of 2-oxo 4-methylthio butanoic acid (OMBA) to Met

(Urrestarazu *et al.*, 1998). To test whether Tam1 of *U. maydis* is also capable of catalysing this reaction, we compared Met production of the wild-type and the *tam1 $\Delta$  strain after growth in the presence of OMBA. Wild-type cells accumulated a twofold higher Met concentration in culture supernatants than the *tam1 $\Delta$  mutant (Fig. 4C). This indicates that Tam1 of *U. maydis* contributes to Met production via amination of OMBA.**

To find out whether OMBA amination by Tam1 affects the Tam1-catalysed conversion of Trp into IP, we conducted feeding experiments of wild-type and *tam1 $\Delta$  strains. In the presence of OMBA, wild-type cells formed a 44-fold higher level of IPA from Trp than without the addition of OMBA (Fig. 4B). In contrast, OMBA addition to the *tam1 $\Delta$  strain did not raise the amount of IPA above the detection limit (Fig. 4B). This confirms that Met production and Trp deamination are linked directly or indirectly by the action of Tam1.**

#### *Biochemical characterization of Tam1*

To confirm whether Tam1 is capable of catalysing the above-mentioned reactions inferred from feeding experiments, we overexpressed and purified the *U. maydis* Tam1 as a His-tagged fusion protein from *E. coli* by nickel affinity chromatography (see *Experimental procedures* and Fig. 5B). Enzyme preparations were incubated for 1 h with different amino acceptors and amino donors, and the concentration of Trp, IPA, Phe and Met was determined by HPLC (Fig. 5A). When incubating purified Tam1 with Trp and PPy, high levels of IPA and Phe were produced, while most of the Trp was consumed (assay condition 1). Additional presence of 2-OG did not significantly increase the amount of IPA or Phe produced or the amount of Trp consumed (assay conditions 2 and 3). When incubating Trp and 2-OG with purified Tam1, only a small amount of IPA was produced (assay condition 4). Together, these results indicate that PPy is preferred over 2-OG as amino acceptor from Trp under the tested conditions.

Our feeding experiments suggested that Tam1 can catalyse the conversion of OMBA to Met. For Aro9 of *S. cerevisiae*, it is known that the conversion of Met to OMBA is coupled to the conversion of Phe to PPy (Urrestarazu *et al.*, 1998). Therefore, we tested the Tam1 enzyme preparation with OMBA and Phe (Fig. 5A, assay condition 7). This reaction led to generation of Met and a decrease in the concentration of Phe. Conversely, when the enzyme preparation was incubated with Met and PPy as substrates (assay condition 6), the concentration of Met decreased while more Phe was generated than in the mock control experiment. This shows that the purified Tam1 is capable of amino group transfer from Phe to OMBA. Therefore, Trp deamination could be indirectly

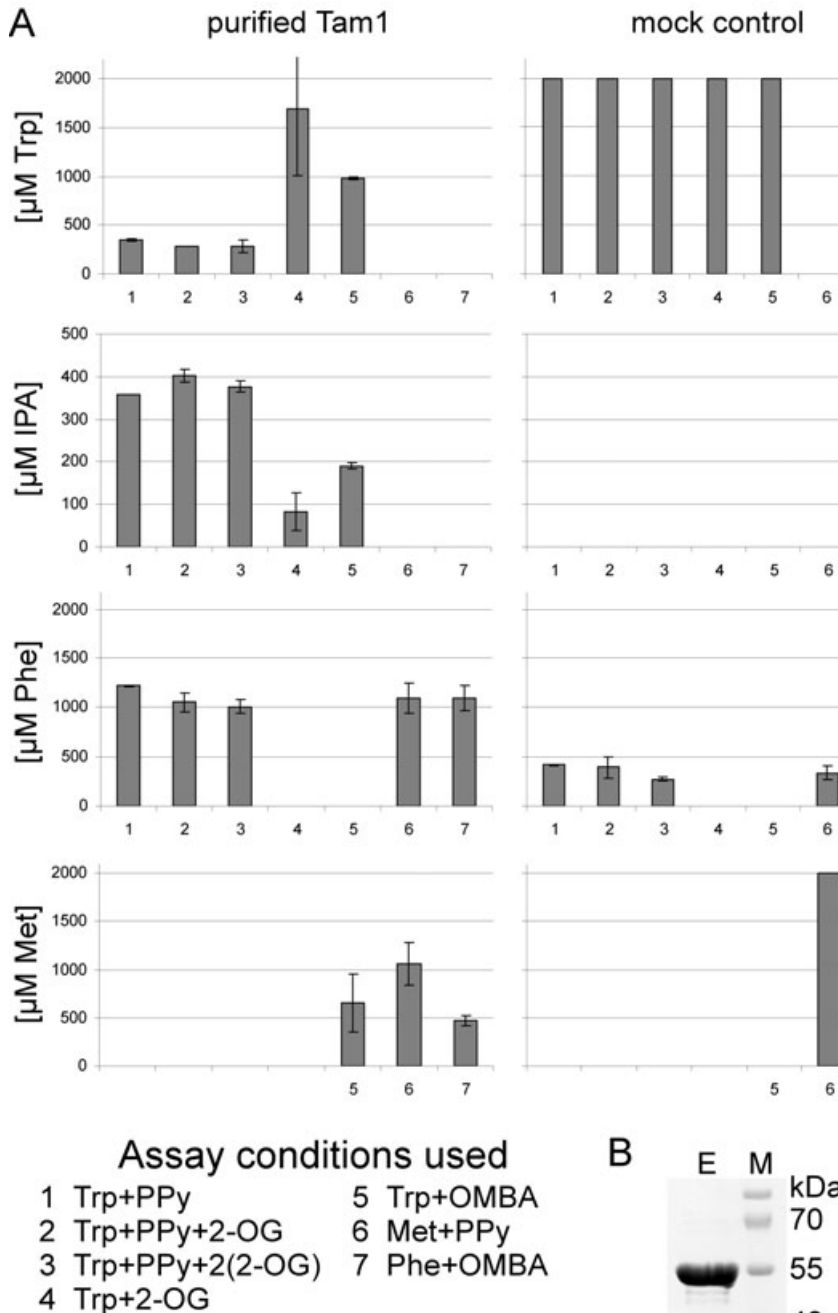
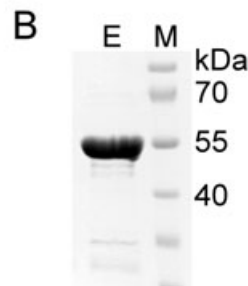


**Fig. 5.** Enzyme activity assays and purification of Tam1.

A. Different substrates (2 mM each) were incubated in different combinations (as indicated below the bar graphs) with purified Tam1, or without enzyme as mock control experiments, for 1 h at 48°C. Amounts of Trp, IPA and Phe in the reaction mixtures were determined by HPLC. Amounts of Met were determined by HPLC-MS/MS only for assay conditions 5, 6 and 7. The concentrations of Trp were calculated by setting the value of the mock control experiments (assay conditions 1–5) to 2 mM. Concentrations of Phe and Met were determined relative to mock control experiments 7 and 6 respectively, which were set to 2 mM. Concentrations of IPA were determined by HPLC as the sum of the amounts of IPA and its degradation product IAA relative to a standard solution. As IPA readily reacts to additional compounds, the concentration of IPA produced is higher than the one determined.

B. Coomassie-stained acrylamide gel showing the final eluting fraction of the purified Tam1 preparation used for the enzyme assays shown in A.



linked to OMBA amination via interconversion of PPy and Phe (see *Discussion* and Fig. 8).

To test whether Tam1 can also directly use OMBA as amino acceptor for the deamination of Trp, we incubated the enzyme preparation with Trp and OMBA (Fig. 5A, assay condition 5). This reaction led to the generation of IPA and Met, showing that OMBA can also serve as direct amino acceptor for the deamination of Trp.

#### *Deletion of Tam1 has no effect on virulence*

As the pigments produced by *M. furfur* are proposed to have a function in symptom development of pityriasis versicolor (Mayser *et al.*, 1998), we tested whether Tam1-mediated pigment formation is required for virulence of *U. maydis* on its host plant maize. To this end, we deleted the *tam1* ORF in the solopathogenic *U. maydis* strain SG200

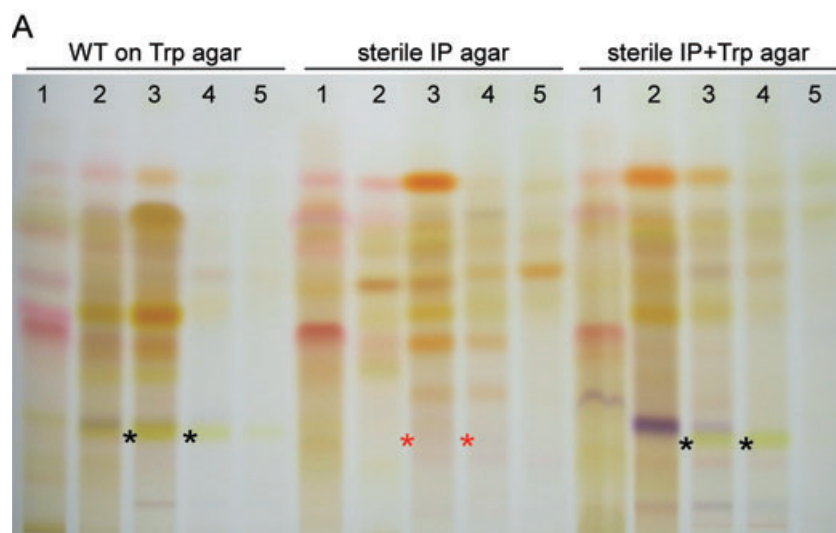


**Fig. 6.** Pigments can form spontaneously in the presence of IP.

A. TLC analysis of fractionated pigment extracts from Trp agar inoculated with the *U. maydis* wild-type strain 521, from sterile IP agar, or from sterile IP + Trp agar. Plates were incubated 3 days at 28°C in the dark prior to pigment extraction. The position of a yellow compound that migrates at a position of PCit is clearly visible in extracts from 521 on Trp agar and in extracts from sterile IP + Trp plates (black stars), but is absent from IP agar (red stars).

B. Presence of indicated compounds in the fractions shown in A was analysed by LC-ESI-MS (PitC, PitB) or MS/MS (PyA, PCit). Trace amounts and not detected represent signal to noise ratios below 30 and below 10 respectively.

**B**

	WT on Trp agar	sterile IP agar	sterile IP + Trp agar
PyA	+	+	+
PitC	+	+	+
PitB	+	nd	+
PCit	+	a	+

a, trace amounts; nd, not detected

(Bölker *et al.*, 1995) to generate two independent deletion mutants, SG200 $\Delta$ tam1#2 and SG200 $\Delta$ tam1#7. These strains as well as the SG200 control strain were used to inoculate 7-day-old seedlings of *Zea mays* cv Early Golden Bantam. For the control strain SG200, 25 of 37 inoculated plants (70%) showed tumour formation, typical symptoms of *U. maydis* infection. For the mutant strains SG200 $\Delta$ tam1#2 and SG200 $\Delta$ tam1#7, 25 of 36 plants (69%) and 26 of 38 (68%) plants, respectively, developed tumours that were comparable in size to those of the control strain. This shows that deletion of *tam1* does not lead to a decrease in virulence of *U. maydis* under the applied conditions. However, as deletion of *tam1* neither abolishes Trp deamination (Fig. 4A) nor pigment production (Fig. 3C) activity completely, we cannot exclude that IP or the pigments contribute to virulence at low concentrations.

#### Indolepyruvate and Trp spontaneously form pigments

To identify genes involved in pigment biosynthesis acting downstream of *tam1*, we examined whether the pigmentation defect of the *tam1* $\Delta$  mutant can be complemented by addition of IP to the growth medium. However, upon supplementation of the medium with purified IP, it rapidly

changed its colour from light yellow to deep red. This indicated that IP could spontaneously form coloured compounds in aqueous solution. Similar observations have been made before (Paris and Magasanik, 1981; Bittinger *et al.*, 2003); however, the generated compounds have to our knowledge never been analysed.

Therefore, we generated pigment extracts from Trp containing agar plates that had been inoculated with *U. maydis* wild-type cells, as well as from sterile agar plates that contained either IP, or Trp and IP. Extracts were fractionated and subjected to TLC analysis. To our surprise, the pigment profiles of the *U. maydis* culture did not show any qualitative differences to the control profile obtained from sterile IP + Trp agar (Fig. 6A). In the profile obtained from sterile IP agar, we observed that a few compounds were absent compared with the other two profiles. One of these compounds is bright yellow and migrates at a position identical to that published for PCit (Fig. 6A, asterisks) (Mayser *et al.*, 2002).

To investigate whether the mixture of spontaneously generated pigments contained the previously identified compounds with biological activity, we analysed all fractions individually by LC-ESI-MS and MS/MS. This analysis showed that PyA, PitC, PitB and PCit occurred not only in the extracts of *U. maydis*-inoculated plates, but

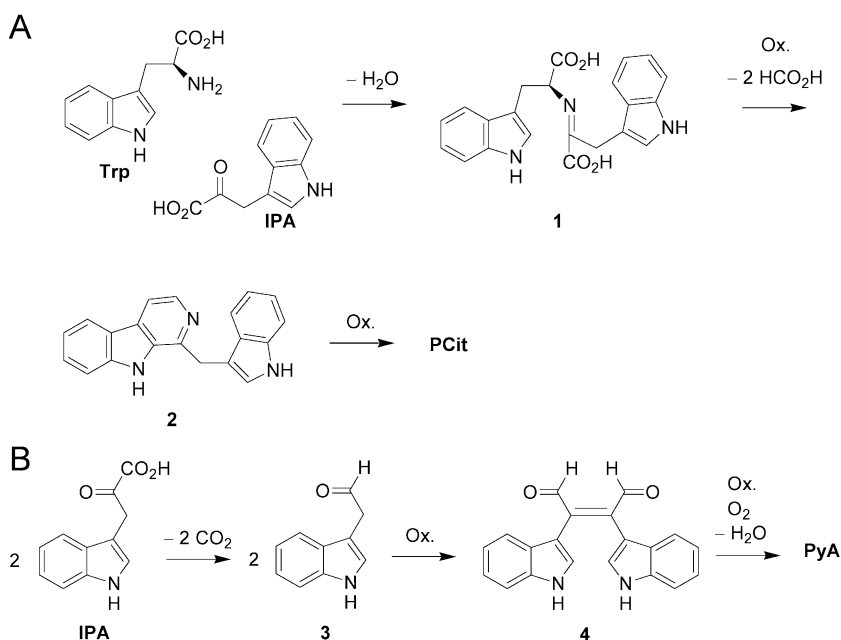


**Fig. 7.** Proposed model for the spontaneous generation of PyA (A) and PCit (B) from IP. Details see text.

also in extracts of sterile IP + Trp agar (Fig. 6B and *Experimental procedures*). In the extract derived from sterile IP agar, we detected PyA and PitC but not PitB and only trace amounts of PCit (Fig. 6B).

To exclude that the generation of the indole pigments involved undefined components present in the agar plates, we performed control experiments and extracted total pigments from sterile aqueous solutions of IP and IP plus Trp 24 h after dissolution of the compounds in water. Extracts were analysed by LC-HR-ESI-MS and LC-HR-ESI-MS/MS. The presence of PyA and PCit, as well as trace amounts of PitC, were confirmed by LC retention times and the MS data that were in good agreement with authentic samples (see *Experimental procedures*). Therefore, the investigated compounds, PyA, PCit and PitC can form spontaneously in an aqueous solution containing IP and Trp. Judged from the striking similarity of the pigment profiles generated from Trp by *U. maydis* or generated spontaneously from IP and Trp (Fig. 6A), it seems highly likely that IP is the precursor for the spontaneous generation of most, if not all, compounds found in pigment extracts from *U. maydis*. In accordance, we have observed that the reaction mixtures (assay conditions 1–5 of Fig. 5A) incubated with the purified Tam1 enzyme preparation turned brown to different extents, proportional to the amounts of IPA detected. Therefore, the biosynthetic pathway leading to Trp-dependent pigment production in *U. maydis* consists of a single enzymatic step, the deamination of Trp to IP catalysed by Tam1.

## Discussion

We embarked on the elucidation of the biochemical pathway leading to the production of novel indole pig-

ments first isolated from *M. furfur*. As *M. furfur* is not genetically amenable, we used the closest sequenced organism, *U. maydis*, as a model. We could show that *U. maydis* produces the same compounds as *M. furfur* when grown on Trp as sole nitrogen source. Using a reverse genetics approach, we identified the Trp aminotransferase Tam1 as the major enzyme responsible for pigment formation from Trp. We then made the unexpected discovery that all subsequent reactions necessary to form the indole pigments PCit, PyA, PitB and PitC from IP occur spontaneously without the action of enzymes, which identifies the Trp aminotransferase as the only biosynthetic enzyme needed for pigment formation from Trp.

The conversion of Trp to coloured compounds by the action of aminotransferases followed by a spontaneous generation of brick-red pigments was first observed in *Klebsiella aerogenes* (Paris and Magasanik, 1981). A similar observation was made when searching for ligands of the AhR of mammalian cells (Bittinger *et al.*, 2003). However, the exact nature of the spontaneously generated pigments or the mechanism of generation remained enigmatic.

### *What is the mechanism for spontaneous production of pigments from IP?*

Pityriacitrin was only generated when the sterile solutions contained both Trp and IP. We propose that the spontaneous generation of PCit commences with a condensation of Trp and IP yielding the imine 1 (Fig. 7A). At this stage, 1 might be twice oxidatively decarboxylated leading under ring formation to the intermediate 2. The decarboxylation reactions are likely catalysed by reactive

oxygen species as has been described for the spontaneous decarboxylation of 2-oxoacids (Vlessis *et al.*, 1990). In the last step, the benzylic CH<sub>2</sub> group might be oxidized to yield PCit (Fig. 7A).

For the generation of PyA, only the presence of IP is required (Fig. 6). Therefore, we propose that IP is non-enzymatically decarboxylated to IAald (3), a reaction that has been shown before (Kaper and Veldstra, 1958; Fig. 7B). At the benzylic position at C-2 of the intermediate 3, a relatively stable radical might be formed. Two of these radicals would then react with each other, leading after a second oxidation to 4. Then, the aldehyde functions of 4 might be oxidized. After formal loss of a molecule of water, PyA is generated (Fig. 7B). In the course of the reactions leading to PCit and PyA, the occurrence of radicals, e.g. the presence of hydroperoxide intermediates, is likely. The involvement of molecular oxygen in this reaction is also suggested through the experiments of Bradfield and co-workers who found that IP was more rapidly converted to pigments when oxygen was bubbled through the solution (Bittinger *et al.*, 2003).

The spontaneous formation of PitC in sterile solutions of Trp and IP should involve both oxidation and reduction reactions, but its exact mechanism, particularly the reactions leading from IP (and Trp) to the proposed precursor 4,5-bis-(1H-indol-3-yl)-cyclopent-4-ene-1,2,3-trione (Irlinger *et al.*, 2004) of the pityriarubins, remains obscure. Whatever the mechanism, spontaneous reaction of Trp and IP yielded PCit, PyA and PitC only as minor constituents in the reaction mixture among at least hundreds of other, so far unknown compounds.

#### *Why are pigment profiles of M. furfur and U. maydis different, if most pigments are generated spontaneously from IP?*

During the initial UV mutagenesis screen, 45 mutants were obtained with a colour different from that of the wild type. Approximately half of the isolated mutants showed a lighter colony colour on Trp plates than the wild type. For some of the mutants that displayed a yellowish colour on Trp plates, individual affected genes could be identified that had a putative role in amino acid metabolism (not shown). Considering the here-presented pathway of pigment biosynthesis from Trp, it is highly likely that the spontaneous reactions following IP generation can also involve other amino acids as well as their respective 2-oxo acids. Of all the generated compounds visible on the TLC plate (Fig. 1C), the identity of only a few compounds is known. It is possible that the other compounds are generated by the reaction of IP with various other amino acids or Trp with other 2-oxoacids, as has been described to occur spontaneously in aqueous solution (Garbe *et al.*, 2000). Relative amounts and pigment composition would

then depend on the availability of different amino acids, which could vary under different conditions, in different environments and between different strains. This could potentially explain the differences in the pigment spectra of *U. maydis* and *M. furfur* (Fig. 1B and C).

#### *Why is the sir1<sup>Δ1054–1499</sup> mutant impaired in pigment formation from Trp?*

During the initial UV-mutagenesis screen aimed at the identification of pigment-deficient mutants, only very few (< 0.05%) mutants with a complete lack of pigment production could be identified. This correlates well with our finding of a single biosynthetic enzyme necessary for pigment production. Surprisingly, in all five identified mutants, the same gene was affected encoding the sulphite reductase Sir1. We could show that strains carrying a deletion of the C-terminal domain of Sir1 were Met auxotrophs. Growth and pigmentation defects could be reverted by the addition of Met, cysteine or sodium sulphide. This indicated that the Sir1 protein is involved in the generation of reduced sulphur compounds and that the strain carrying a deletion of the C-terminal domain of Sir1 might be affected in biosynthesis of sulphur-containing amino acids.

We could show that the only enzyme necessary for pigment production from Trp is Tam1. A hint that Tam1 could be the link between pigment production and sulphur metabolism stemmed from work on Aro8 and Aro9 of *S. cerevisiae*. Both Aro8 and Aro9 contribute to amino group transfer from Met to PPy (Urrestarazu *et al.*, 1998). Feeding experiments indicated that Tam1 of *U. maydis* can also use OMBA as substrate for the generation of Met (Fig. 4C). This could be confirmed by *in vitro* activity assays using purified Tam1 (Fig. 5A). As in *S. cerevisiae*, amination of OMBA by Tam1 could be coupled to the deamination of Phe to PPy. Interestingly, the *in vitro* experiments showed that Tam1 can also couple amination of OMBA directly to Trp deamination (Fig. 5A). Therefore, there are two avenues linking sulphur metabolism to pigment production (Fig. 8). The first avenue is the capacity of Tam1 to directly use OMBA as amino acceptor for Trp deamination (reaction 1, Fig. 8). The second path couples OMBA amination indirectly to Trp deamination. In this circuit, Trp deamination to IP by Tam1 is coupled to the amination of PPy to Phe (reaction 2, Fig. 8). IP accumulation would then depend on the regeneration of PPy by the Tam1-catalysed amino transfer from Phe to OMBA (reaction 3, Fig. 8). In the *sir1*<sup>Δ1054–1499</sup> mutant, OMBA (whose presence is dependent on a functional sulphite reductase) is not present in sufficient quantities to either serve as a direct amino acceptor or to support PPy recycling. Thus, pigment formation is stalled as soon as available amino acceptors are exhausted. Congruently,

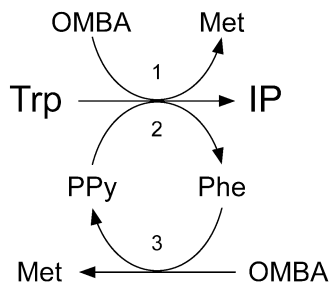


**Fig. 8.** Tam1-catalysed reactions link Trp conversion to IP both directly and indirectly to amination of OMBA. Tam1 can directly use OMBA as amino acceptor for Trp deamination (reaction 1). Trp deamination is also indirectly dependent on OMBA amination via amino group transfer from Trp to PPy (reaction 2) and PPy regeneration by Tam1-catalysed amino group transfer from Phe to OMBA (reaction 3). In the absence of OMBA, PPy concentrations are limiting and determine the amount of IP that can be formed by Tam1 from an excess of Trp.

the addition of PPy to Trp plates restored the ability of *sir1Δ*<sup>1054–1499</sup> mutants to form pigments (Fig. 2E).

#### Could spontaneously generated compounds have important biological effects?

It is well known that aqueous Trp solutions contain spontaneously generated photoproducts. One of them, 6-formylindolo[3,2-*b*]carbazole (FICZ), has been well characterized (Rannug *et al.*, 1995) and shown to bind very efficiently to the AhR of mammalian cells (Wei *et al.*, 1998; Bergander *et al.*, 2004). FICZ binding to the AhR leads to translocation of the AhR from the cytoplasm to the nucleus (Okey *et al.*, 1994), where it induces the generation of high levels of CYP1A1 (Fritsche *et al.*, 2007). CYP1A1 is a cytochrome P450 mono-oxygenase with an important role in chemical carcinogenesis (Nebert and Dalton, 2006). AhR-mediated CYP1A1 activity has been shown to be stimulated by spontaneous production of FICZ in culture medium (Oberge *et al.*, 2005). In line with this finding, we could also demonstrate presence of FICZ in extracts of sterile plates containing Trp and IP (see *Experimental procedures*).

In addition to FICZ, further compounds identified in extracts from *M. furfur* grown on Trp have the potential to bind to the AhR. Malassezin has already been described to function as an AhR agonist (Wille *et al.*, 2001), while a number of identified indolocarbazoles have a high structural similarity to FICZ (Irlinger *et al.*, 2005). These are also expected to bind AhR, as the AhR binds to polycyclic planar aromatic hydrocarbons (Bittinger *et al.*, 2003).

Interestingly, Bradfield and co-workers could show that IP is a proagonist of the AhR and that IP spontaneously reacts to a large number of compounds that could function in AhR activation (Bittinger *et al.*, 2003). They observed that longer incubation of IP in aqueous solution resulted in a darker colour of the solutions, and that darker solutions

were more potent in activation of AhR (Bittinger *et al.*, 2003). Recently, FICZ was demonstrated to serve as one of the long-sought-for cytoplasmic ultraviolet B (UV B)-stress signalling molecules that induce a DNA damage independent UV B-stress response by binding to the AhR (Fritsche *et al.*, 2007). It is conceivable that *M. furfur* converts Trp into IP on human skin and that IP then spontaneously reacts to agonists of the AhR. Agonist binding to the AhR could result in an activation of the AhR-mediated UV B-stress response pathway and could, potentially, contribute to the observed UV resistance of lesions of pityriasis versicolor. In this respect, it is interesting that IPA was patented as a potent sun protection agent (Politi *et al.*, 1992). Here, also, protection could be indirect by degradation products generated spontaneously from IPA.

The generation of chromopyrrolic acid, a precursor of the anti-tumourigenic indolocarbazoles staurosporine and rebeccamycine, by oxidative dimerization of oxidized Trp, is dependent on oxygen but independent of the presence of enzymes once IPA is formed (Balibar and Walsh, 2006; Howard-Jones and Walsh, 2006). In addition, non-enzymatic reactions contribute to biosynthesis of staurosporine and rebeccamycine following the formation of chromopyrrolic acid (Howard-Jones and Walsh, 2007). Congruently, we also found chromopyrrolic acid among the compounds that are spontaneously generated from Trp and IP in extracts from sterile plates (see *Experimental procedures*).

Another important molecule that can spontaneously form from IP is IAA (Kaper and Veldstra, 1958). IAA functions in all aspects of plant growth and development (Teale *et al.*, 2006). In plants, the enzyme IP decarboxylase has been suggested to act as a regulatory unit to accelerate IP conversion when needed (Koga, 1995). However, most pathways leading to IAA production do not go via IP (Teale *et al.*, 2006), possibly to avoid spontaneous and untimely generation of this important plant growth hormone.

The level of IAA in tumour tissue of *U. maydis*-infected maize plants is increased, and IAA production by *U. maydis* has been proposed to contribute to tumour formation (Wolf, 1952). IAA biosynthesis has been suggested to involve the IAAld dehydrogenases *lad1* and *lad2*; however, *lad1Δlad2Δ* double deletion mutants were unaffected in virulence (Basse *et al.*, 1996; Reineke *et al.*, 2008). Deletion of *tam1* did not reduce virulence of a solopathogenic *U. maydis* strain. In line with this result, deletion of *tam1* in strains lacking *lad1* and *lad2* did also not affect virulence (Reineke *et al.*, 2008). However, in these mutants the IAA concentration in tumours was reduced, while the absence of *lad1* and *lad2* did not affect host IAA levels (Reineke *et al.*, 2008). This may indicate that Tam1-catalysed deamination of Trp to IP also plays a role in the generation of IAA in *U. maydis*-infected plant tissue.

It is emerging that spontaneously generated compounds influence biological systems in various ways. This is exemplified by the spontaneous formation of FICZ from Trp that functions as an important signalling molecule, by spontaneous reactions contributing to the generation of anti-tumourigenic substances, and by spontaneous generation of the plant growth hormone IAA from IP. Thus, spontaneously generated compounds can have a severe impact on various fundamental processes. To date, this is a fairly unexplored field of study that clearly merits closer attention.

## Experimental procedures

### Strains and growth conditions and plant infections

The *E. coli* K12 strains DH5 $\alpha$  (Gibco BRL, Gaithersburg, Maryland, USA) and Top10 (Invitrogen, Paisley, UK) were used as hosts for cloning purposes and cultivated in 2xYT (Sambrook *et al.*, 1989) at 37°C with shaking or on YT solidified with agar (13 g l<sup>-1</sup>). Ampicillin was used at a concentration of 100  $\mu$ g ml<sup>-1</sup>.

*Ustilago maydis* wild-type strain 521 (R. Holiday) was used as reference strain. For plant infection experiments, the solo-pathogenic *U. maydis* strain SG200 (Bölker *et al.*, 1995) was used. *U. maydis* strains were grown at 28°C in YEPS light [yeast extract (10 g l<sup>-1</sup>), bacto-pepton (4 g l<sup>-1</sup>), sucrose (4 g l<sup>-1</sup>)], in complete medium (CM) (Holliday, 1974) containing glucose (10 g l<sup>-1</sup>), or on potato dextrose agar (Difco, Lawrence, Kansas, USA).

*Malassezia furfur* strain CBS 1878T was grown on modified Dixon agar (mDixon) (Gueho *et al.*, 1996) at 32°C. For pigment production, *M. furfur* was smeared onto Trp agar plates (see below) and incubated for 4 weeks in the dark at 32°C.

Hygromycin B was from Roche (Mannheim, Germany), phleomycin from Cayla (Toulouse, France) and carboxin from Riedel de Haen (Seelze, Germany). All other chemicals were of analytical grade and were obtained from Sigma-Aldrich (Steinheim, Germany) or Merck (Darmstadt, Germany).

Plant infections of the corn variety Early Golden Bantam (Olds Seeds, Madison, WI) were performed essentially as described previously (Gillissen *et al.*, 1992).

### Isolation and analysis of indole pigments from agar plates

Pigment extraction and fractionation of cultures of *M. furfur* were done as described (Mayser *et al.*, 2007). Pigment extraction and compound purification leading to the initial identification of pigments produced by *U. maydis* were done as described (Mayser *et al.*, 2007). UV spectra were recorded on a Varian Cary 100 Bio UV-Vis spectrometer (Varian, Darmstadt, Germany; PCit: 1.0 mg,  $R_t$  = 143–150 min; PyA: 0.47 mg,  $R_t$  = 130–140 min; MI: 7.1 mg,  $R_t$  = 60–100 min; MA: 0.78 mg,  $R_t$  = 64–75 min; PitC: trace amounts,  $R_t$  = 112–120 min).

Nuclear magnetic resonance spectra were recorded with a Bruker DMX 500 spectrometer (<sup>1</sup>H at 500.11 MHz; Bremen,

Germany). Chemical shifts were determined relative to the solvent CD<sub>3</sub>OD ( $\delta_H$  3.31 p.p.m) as internal standards. EI-MS spectra were obtained with a Thermo Electron DSQ (Austin, Texas, USA) instrument equipped with direct insertion probe using EI at 70 eV. LC-HR-ESI-MS and LC-HR-ESI-MS/MS spectra were obtained with a Thermo Scientific LTQ-Orbitrap mass spectrometer (Austin, Texas, USA). The spectrometer was operated in positive mode (one spectrum s<sup>-1</sup>; mass range: 50–1000) with nominal mass resolving power of 60 000 at  $m/z$  = 400 with a scan rate of 1 Hz with automatic gain control to provide high-accuracy mass measurements within 2 p.p.m. deviation using polydimethylcyclsiloxane <[(CH<sub>3</sub>)<sub>2</sub>SiO]<sub>6</sub>,  $m/z$  = 445.120025> as internal lock mass. The spectrometer was equipped with a Dionex HPLC system Ultimate 3000 consisting of pump, UV detector ( $\lambda$  = 254 nm), Flow Manager and autosampler (injection volume 0.5  $\mu$ l; Idstein, Germany). Nitrogen was used as sheath gas (6 arbitrary units) and helium served as the collision gas. The separations were performed with a Gemini C-18 column (Phenomenex, Aschaffenburg, Germany; 3  $\mu$ m, 0.3  $\times$  150 mm) using the following gradient programme: 2 min at 89.9% H<sub>2</sub>O/10% MeCN/0.1% HCO<sub>2</sub>H, then within 8 min linear to 99.9% CH<sub>3</sub>CN/0.1% HCO<sub>2</sub>H, then 10 min at 99.9% CH<sub>3</sub>CN/0.1% HCO<sub>2</sub>H, flow rate: 4  $\mu$ l min<sup>-1</sup>.

The compounds PCit, PyA, MI, MA and PitC were identified by comparison of the spectroscopic data given below with published data (Brenner *et al.*, 1988; Mayser *et al.*, 2002; Irlinger *et al.*, 2004; 2005).

**PCit:** Yellow solid. <sup>1</sup>H NMR (500 MHz, CD<sub>3</sub>OD, 297 K):  $\delta$  = 7.27–7.33 (m, 3 H, H-6, H-5', H-6'), 7.49–7.52 (m, 1 H, H-7'), 7.60 (dd, <sup>3</sup> $J_{HH}$  = 8.1 Hz, <sup>3</sup> $J_{HH}$  = 8.2 Hz, H-7), 7.72 (d, 1 H, <sup>3</sup> $J_{HH}$  = 8.2 Hz, H-8), 8.24 (d, 1 H, <sup>3</sup> $J_{HH}$  = 7.9 Hz, H-5), 8.28 (d, 1 H, <sup>3</sup> $J_{HH}$  = 5.0 Hz, H-4), 8.52 (d, 1 H, <sup>3</sup> $J_{HH}$  = 5.0 Hz, H-3), 8.59–8.62 (m, 1 H, H-4'), 9.05 (s, 1 H, H-2'). EI-MS:  $m/z$  (%) = 311 (67) [M]<sup>+</sup>, 294 (100) [M – NH<sub>3</sub>]<sup>+</sup>, 282 (52), 255 (6), 166 (12), 155 (34), 144 (32), 127 (6), 116 (18), 89 (10).

**PyA:** Red solid. <sup>1</sup>H NMR (500 MHz, CD<sub>3</sub>OD, 297 K):  $\delta$  = 6.65 (dd, 1 H, <sup>3</sup> $J_{HH}$  = 7.3 Hz, <sup>3</sup> $J_{HH}$  = 8.0 Hz, H-5), 6.86 (d, 1 H, <sup>3</sup> $J_{HH}$  = 8.0 Hz, H-4), 7.02 (dd, 1 H, <sup>3</sup> $J_{HH}$  = 7.3 Hz, <sup>3</sup> $J_{HH}$  = 8.0 Hz, H-6), 7.37 (d, 1 H, <sup>3</sup> $J_{HH}$  = 8.0 Hz, H-7), 7.85 (s, 1 H, H-2). EI-MS:  $m/z$  (%) = 328 (96) [M]<sup>+</sup>, 300 (3) [M – CO]<sup>+</sup>, 284 (7) [M – CO<sub>2</sub>]<sup>+</sup>, 256 (100) [M – CO – CO<sub>2</sub>]<sup>+</sup>, 227 (14), 200 (10), 150 (6), 144 (20), 128 (14), 114 (16), 101 (12).

**MI:** Yellow solid. <sup>1</sup>H NMR (500 MHz, CD<sub>3</sub>OD, 297 K):  $\delta$  = 2.93 (dd, 1 H, <sup>2</sup> $J_{HH}$  = 16.0 Hz, <sup>3</sup> $J_{HH}$  = 10.9 Hz, H-1), 3.53 (d, 1 H, <sup>3</sup> $J_{HH}$  = 16.0 Hz, H-1), 4.58 (d, 1 H, <sup>3</sup> $J_{HH}$  = 10.9 Hz, H-2), 5.31 (s, 1 H, H-5), 6.65 (s, 1 H, H-2'), 6.99 (dd, 1 H, <sup>3</sup> $J_{HH}$  = 7.2 Hz, <sup>3</sup> $J_{HH}$  = 7.9 Hz, H-5'), 7.01 (dd, 1 H, <sup>3</sup> $J_{HH}$  = 7.0 Hz, <sup>3</sup> $J_{HH}$  = 7.9 Hz, H-9), 7.09–7.14 (m, 2 H, H-6', H-8), 7.31–7.33 (m, 2 H, H-6', H-7), 7.47 (d, 1 H, <sup>3</sup> $J_{HH}$  = 7.9 Hz, H-10), 7.68 (d, 1 H, <sup>3</sup> $J_{HH}$  = 7.9 Hz, H-4').

LC-HR-ESI-MS:  $m/z$  = 360.1343 [M + H]<sup>+</sup>, calculated for C<sub>21</sub>H<sub>18</sub>N<sub>3</sub>O<sub>3</sub> 360.1348.

**MA:** Yellow solid. <sup>1</sup>H NMR (500 MHz, CD<sub>3</sub>OD, 297 K):  $\delta$  = 7.10 (dd, 1 H, <sup>3</sup> $J_{HH}$  = 6.7 Hz, <sup>3</sup> $J_{HH}$  = 7.7 Hz, H-8), 7.21 (dd, 1 H, <sup>3</sup> $J_{HH}$  = 7.1 Hz, <sup>3</sup> $J_{HH}$  = 7.7 Hz, H-2), 7.37–7.43 (m, 2 H, H-3, H-9), 7.47 (d, 1 H, <sup>3</sup> $J_{HH}$  = 7.7 Hz, H-10), 7.53 (d, 1 H, <sup>3</sup> $J_{HH}$  = 8.0 Hz, H-4), 8.15 (d, 1 H, <sup>3</sup> $J_{HH}$  = 7.7 Hz, H-1), 8.39 (s, 1 H, H-12), 8.59 (d, 1 H, <sup>3</sup> $J_{HH}$  = 6.7 Hz, H-7).

LC-HR-ESI-MS:  $m/z = 329.0919$   $[M + H]^+$ , calculated for  $C_{20}H_{13}N_2O_3$  329.0926.

**PitC:** Red solid. LC-HR-ESI-MS:  $m/z = 526.1397$   $[M + H]^+$ , calculated for  $C_{32}H_{20}N_5O_5$  526.1403.

For generation of all other pigment extracts, *U. maydis* strains were pre-cultured in YEPS light to an  $OD_{600}$  of 1.0, and concentrated by centrifugation and resuspension in water to an  $OD_{600}$  of 3.0. Except for the sterile control plates, all plates were inoculated with 500  $\mu$ l of concentrated cells. For the experiments analysing pigment production of *U. maydis* aminotransferase mutants, and of sterile control plates, pigments were extracted from 35 agar plates containing agar (20 g l<sup>-1</sup>; Merck, Darmstadt, Germany), glucose (50 mM), Tween 80 (3% v/v), and either Trp (15 mM) (Trp agar), IP (3 mM) (IP agar), or IP (3 mM) and Trp (15 mM) (IP + Trp agar). For the experiments analysing the sulphite reductase mutants, pigments were extracted from five Trp agar plates each, lacking or containing 1.3 mM Met. All plates were incubated in the dark at 28°C for 3 days.

The entire culture medium along with the biomass was collected, pured and then extracted with EtOAc (Merck, Darmstadt, Germany) for 12 h. The extract was filtered through glass wool, the filtrate evaporated to dryness under reduced pressure using a rotary evaporator (Heidolph, Schwalbach, Germany), and the residue dissolved in methanol (MeOH). For the experiments analysing the sulphite reductase mutants, crude extracts were separated from Tween 80 by gel chromatography with a Sephadex LH-20 column (20  $\times$  1.5 cm) and MeOH as eluent. For the experiments analyzing pigment production of aminotransferase mutants, and of sterile control plates, crude extracts were fractionated by gel chromatography with a Sephadex LH-20 column (60  $\times$  3 cm) and MeOH as eluent into seven fractions of 200 ml each and evaporated to dryness. Residues were dissolved in 2 ml MeOH and 10  $\mu$ l cm<sup>-1</sup> was applied to TLC silica gel 60 plates (20  $\times$  20  $\times$  1 mm, Merck, Darmstadt, Germany) with a Linomat IV (Camag, Berlin, Germany). The plates were developed for 45 min with the solvent system toluene/HCO<sub>2</sub>Et/HCO<sub>2</sub>H 10:5:3 (v/v/v) (PCit:  $R_f = 0.18$ ; PyA:  $R_f = 0.46$ ; MI:  $R_f = 0.38$ ; MA:  $R_f = 0.27$ ; PitC:  $R_f = 0.38$ ) and directly documented by photography (Camag).

Fractions were further analysed by LC-ESI-MS and LC-ESI-MS/MS using a Varian system consisting of two pumps, a degasser, an autosampler, a diode array detector and a column oven (Varian, Darmstadt, Germany). The analytes were separated on a polar modified RP-18 column (Synergi Fusion RP 80 A column; 4  $\mu$ m, 100  $\times$  2 mm i.d.; Phenomenex, Aschaffenburg, Germany). The column was maintained at a temperature of 40°C. The flow rate was set to 0.2 ml min<sup>-1</sup>, the injection volume was 10  $\mu$ l. Solvent A was water with 7 mM acetic acid, solvent B was MeOH with 7 mM acetic acid. Samples were separated as follows in a binary gradient: 0–1 min 10% B, 1–21 min 10–98% B, followed by washing and re-equilibration steps. Diode array detection was performed in a range of 200–500 nm with the detector being connected upstream of the mass spectrometer. For MS detection, a Varian 1200 triple quadrupole was used with positive and negative ESI (Varian, Darmstadt, Germany). Gas flow and temperature were 200°C and 20 psi. Needle, shield and capillary voltage were –3500/–600/–40 V for nega-

tive ESI, and 5000/250/80 V for positive ESI. Fragmentation was performed in a collision cell with argon gas. System control was done by Varian MS Workstation 6.5 (Varian, Darmstadt, Germany). Quantitative determination was performed in single reaction monitoring for PitB and PitC, and multiple reaction monitoring for PyA and PCit respectively.

Chromopyrrolic acid was identified from combined fractions of extracts derived from sterile plates containing Trp and IP by LC-ESI-MS/MS fragmentation of the parent ion  $[M - H]^-$  with  $m/z$  384 to the fragment ions  $m/z$  340  $[M - CO_2]^-$  and  $m/z$  296  $[M - 2CO_2]^-$  according to literature (Nishizawa *et al.*, 2006) under the conditions described above with a retention time of 17.12 min.

6-formylindolo[3,2-*b*]carbazole was identified from combined fractions of extracts derived from sterile plates containing Trp and IP by LC-ESI-MS/MS fragmentation of the parent ion  $[M + H]^+$  with  $m/z$  285 to the fragment ion 255  $[M - CHOH + H]^+$  under the conditions described above with a retention time of 22.5 min (Fritsche *et al.*, 2007).

The compounds PCit, PyA, PitC and PitB were identified by comparison of the spectroscopic data given below with published data and comparison with authentic samples (Brenner *et al.*, 1988; Mayser *et al.*, 2002; Irlinger *et al.*, 2004; 2005).

**PCit:** UV-Vis (MeOH/H<sub>2</sub>O):  $\lambda = 315, 389$  nm. LC-ESI-MS:  $R_t = 20.3$  min,  $m/z = 312$   $[M + H]^+$ . LC-ESI-MS/MS (parent ion  $m/z = 312$ ):  $m/z = 195$   $[M + H - indole]^+$ , 167  $[M + H - indole-3-carbaldehyde]^+$ .

**PyA:** UV-Vis (MeOH/H<sub>2</sub>O):  $\lambda = 277, 389, 462$  nm. LC-ESI-MS:  $R_t = 18.3$  min,  $m/z = 327$   $[M - H]^-$ . LC-ESI-MS/MS (parent ion  $m/z = 327$ ):  $m/z = 283$   $[M - CO_2H]^-$ , 255  $[M - CO_2H - CO]^-$ .

**PitC:** UV-Vis (MeOH/H<sub>2</sub>O):  $\lambda = 277, 323, 394, 462$  nm. LC-ESI-MS:  $R_t = 16.5$  min,  $m/z = 524$   $[M - H]^-$ . LC-ESI-MS/MS (parent ion  $m/z = 524$ ):  $m/z = 480$   $[M - CO_2H]^-$ , 452  $[M - CO_2H - CO]^-$ .

**PitB:** UV-Vis (MeOH/H<sub>2</sub>O):  $\lambda = 277, 446$  nm. LC-ESI-MS:  $R_t = 15.2$  min,  $m/z = 523$   $[M - H]^-$ . LC-ESI-MS/MS (parent ion  $m/z = 523$ ):  $m/z = 479$ .

#### *Spontaneous generation of indole alkaloids from IP alone and from IP and Trp in aqueous solution*

Indolepyruvate (30.48 mg, 0.15 mmol) or IP (30.48 mg, 0.15 mmol) plus Trp (30.63 mg, 0.15 mmol) was suspended in a mixture of H<sub>2</sub>O (10 ml) and Tween 80 (50  $\mu$ l) and stirred vigorously. After 24 and 72 h, one half (5 ml) of the reaction mixture was removed and extracted three times with EtOAc (20 ml for each extraction). The combined organic layers were dried (Na<sub>2</sub>SO<sub>4</sub>) and the solvent was removed at 40°C *in vacuo*. The residue was dissolved in MeOH (1 ml) and separated with MeOH on Sephadex LH-20 (column dimensions: 10  $\times$  20 mm). After collection of five coloured fractions, the solvent was removed at 40°C *in vacuo* from each sample and each residue was analysed by LC-HR-ESI-MS and LC-HR-ESI-MS/MS. LC-HR-ESI-MS and LC-HR-ESI-MS/MS spectra were obtained with a Thermo Scientific LTQ-Orbitrap mass spectrometer (Austin, Texas, USA). The LC retention times and the MS data were in good agreement with authentic samples.

Specifications of compounds in solution of IP:

**PyA:** LC-HR-ESI-MS:  $R_t = 11.45$  min,  $m/z = 329.0920$   $[M + H]^+$ , calculated for  $C_{20}H_{13}N_2O_3$  329.0926.

Specifications of compounds in solution of IP and Trp:

**PcIt:** LC-HR-ESI-MS:  $R_t = 14.96$  min,  $m/z = 312.1125$   $[M + H]^+$ , calculated for  $C_{20}H_{14}N_3O$  312.1137. LC-HR-ESI-MS/MS (parent ion  $m/z$  312, 35 eV):  $m/z$  (%) = 213.0649 (17)  $[C_{12}H_9O_2N_2]^+$ , 195.0544 (55)  $[C_{12}H_7ON_2]^+$ , 185.0701 (18)  $[C_{11}H_9ON_2]^+$ , 167.0596 (100)  $[C_{11}H_7N_2]^+$ .

**PyA:** LC-HR-ESI-MS:  $R_t = 11.45$  min,  $m/z = 329.0918$   $[M + H]^+$ , calculated for  $C_{20}H_{13}N_2O_3$  329.0926, LC-HR-ESI-MS/MS (parent ion  $m/z$  329, 35 eV):  $m/z$  (%) = 311.0802 (72)  $[C_{20}H_{11}N_2O_2]^+$ , 301.0959 (45), 285.1010 (100)  $[C_{19}H_{13}N_2O]^+$ , 273.1007 (12)  $[C_{18}H_{13}N_2O]^+$ , 257.1059 (5)  $[C_{18}H_{13}N_2]^+$ .

**PitC:** LC-HR-ESI-MS:  $R_t = 13.18$  min,  $m/z = 526.1402$   $[M + H]^+$ , calculated for  $C_{32}H_{20}N_3O_5$  526.1403. LC-HR-ESI-MS/MS (parent ion  $m/z$  526, 35 eV):  $m/z$  (%) = 498.1436 (17)  $[C_{31}H_{20}N_3O_4]^+$ , 482.1486 (100)  $[C_{31}H_{20}N_3O_3]^+$ , 464.1378 (16)  $[C_{31}H_{18}N_3O_2]^+$ , 454.1540 (69)  $[C_{30}H_{20}N_3O_2]^+$ , 438.1588 (10)  $[C_{30}H_{20}N_3O]^+$ , 426.1589 (22)  $[C_{29}H_{20}N_3O]^+$ , 409.0805 (9)  $[C_{24}H_{13}N_2O_5]^+$ , 381.0857 (12)  $[C_{23}H_{13}N_2O_4]^+$ , 353.0902 (5)  $[C_{22}H_{13}N_2O_3]^+$ , 337.0959 (12)  $[C_{22}H_{13}N_2O_2]^+$ .

#### Cloning procedures, constructs and generation of deletion mutants

Molecular methods followed described protocols (Sambrook *et al.*, 1989). DNA isolation from *U. maydis* was carried out as described (Hoffman and Winston, 1987). *U. maydis* mutants were generated by transformation of protoplasts (Schulz *et al.*, 1990) with linear polymerase chain reaction (PCR)-generated deletion constructs (see Table 1). Single-copy integration of all constructs as well as homologous recombination were verified for all strains by Southern analysis. Deletion constructs were prepared using a PCR-based method (Kämper, 2004).

**tam1 $\Delta$  construct.** To generate a fragment for the deletion of *tam1* (um01804), the 5'- and 3'-flanking regions of *tam1* were amplified with primer combinations oJS368 (ATAATG GCCACGTGGGCCAGCCGCAAAGTCAATAAGC)/oJS369 (ATAATGGCCTGAGTGGCCGGTTTGACAGGGAGGATATTGG) and oJS370 (ATCTAGGCCATCTAGGCCTGAGCTC GCTTAAATGG)/oJS371 (ATAATGGCCACGTGGGCCGATTTCATACTCGCGGAACC), respectively, prior to digestion with SfiI and ligation to the 1.9 kb SfiI carboxin-resistance cassette of plasmid pMF1-c (Brachmann *et al.*, 2004). The deletion construct was amplified with the nested primers oJS372 (CCGAATTGTGCCGGATTGC) and oJS373 (ATTACGCGGCTCGTTTCAGG).

**tam2 $\Delta$  construct.** The 5'- and 3'-flanking regions of *tam2* were amplified with primer combinations oTam1 (GCTCGTCTGGGGTACCATTGCAAG)/oTam2 (CACGGCCT GAGTGGCCTGGCGATGTGGCCGAGGACATC) and oTam3 (GTGGCCATCTAGGCCGGCTCCAGATTCTGC CTAG)/oTam4 (CATGTCAACAGACCCAGCTGC), respec-

tively, prior to digestion with SfiI, ligation to the 2.4 kb SfiI phleomycin-resistance cassette of pMF1-p (Brachmann *et al.*, 2004) and cloning into pCRZeroBlunt (Invitrogen) to yield pphle8. The identity of the cloned flanks was verified by sequencing. The *tam2* deletion construct was amplified from pphle8 using nested primers oTam1ne (GACTCGGG GCACTCTCCAAGTC) and oTam4ne (GAGAGCATCACTCA GCTCTCG).

**tam2 $\Delta$ nat construct.** The *tam2 $\Delta$ nat* construct was prepared essentially as described for the *tam2 $\Delta$*  construct, except that the SfiI-digested flanks were ligated to the 1.4 kb nourseo-thricin cassette of pMF1-n (Brachmann *et al.*, 2004) and cloned into pCRZeroBlunt (Invitrogen) to yield ptam2ko\_nat. The identity of the cloned flanks was verified by sequencing and the *tam2* deletion construct was amplified from ptam2ko\_nat as described above.

**sir1 $\Delta$ <sup>1054-1499</sup> construct.** To generate a fragment for the deletion of the C-terminal domain of *sir1* (um02922), the 5'- and 3'-flanking regions were amplified with primer combinations oKZ50 (ATCTAGGCCACGTGGCCATGCTCAGGCTGCT CACAAG)/oKZ51 (ATACTGGCCATCTAGGCCGGATTGGG CGAGCACATGAC) and oJS302 (ACTATGGCCTGAGT GGCCGTGCATCTTCGGCATGATCG)/oJS303 (ATATAGGC CCACGTGGCCATGGATGGCACGTTGATCG), respectively, prior to digestion with SfiI and ligation to the 2.4 kb SfiI hygromycin-resistance cassette of plasmid pMF1-h (Brachmann *et al.*, 2004). The deletion construct was amplified with the nested primers oKZ52 (AGTTTCTCCACGCACTGATG) and oJS305 (GTTGCCCAAAGAAGTGAACG).

#### UV mutagenesis and complementation

In two independent experiments, *U. maydis* 521 cells ( $8 \times 10^4$  per plate) were streaked on a total of 400 Trp agar plates lacking Tween 80 and exposed to a UV dose of 55–65 mJ/cm<sup>2</sup>, corresponding to a survival rate of about 1%, using the Stratalinker UV crosslinker (Stratagene). Plates were incubated in the dark at 28°C for 12 days and screened for colonies with white, yellow or black colony colour. Selected colonies were streaked on Trp plates and one individual colony each was used for further analysis. Colony colour of the obtained mutants was compared with that of the progenitor strain after growth for 7 days on Trp plates at 28°C in the dark. Mutants displaying a colony colour visibly different from that of the wild type were retained.

For complementation, protoplasts of selected mutants were transformed with a genomic library (8 kb fragments; F. Kaffarnik, J. Kämper and R. Kahmann, unpublished) of *U. maydis* strain 521 in the autonomously replicating plasmid pNEBUH (G. Weinzierl, unpublished) that confers resistance to the antibiotic hygromycin. Transformed protoplasts were regenerated on Trp agar containing sorbitol (1 M) and hygromycin ( $150 \mu\text{g ml}^{-1}$ ) at 28°C in the dark. Transformants with restored pigment formation capacity were streaked on Trp plates containing hygromycin ( $150 \mu\text{g ml}^{-1}$ ), and a single colony was used for preparation of total DNA according to the protocol of Schulz (Schulz *et al.*, 1990). Total DNA was dialysed for at least 20 min on nitrocellulose membranes

(0.025 µm, Millipore) against 10% glycerol and used for transformation of electrocompetent *E. coli*. Plasmids of ampicillin-resistant transformants were isolated and analysed by restriction digest. Plasmids giving rise to different restriction patterns were analysed by sequencing using the sequencing facility of the Max-Planck-Institute for Plant Breeding, Cologne, Germany.

To test complementation of 521sir1Δ<sup>1054–1499</sup> by amino acceptors, an overnight culture of 521sir1Δ<sup>1054–1499</sup>#11 in YEPS light was washed 20 times with the double amount of water, followed by an additional wash step at 4°C for 14 h without shaking. Cells were resuspended in water to an OD of 2 and 1 ml each was plated on a Trp agar without or with 1 mM PPy.

### Feeding experiments

Strains were pre-cultured in CM containing glucose (1%) for 24 h at 28°C and then centrifuged at 13 000 r.p.m. for 2 min. Cell pellets were resuspended in sterile water to an OD<sub>600</sub> of 3.0. Cell suspensions were added to CM containing glucose (10 g l<sup>-1</sup>) and Trp (5 mM) to a final OD<sub>600</sub> of 0.1 and supplemented with either PPy (1 mM), 2-OG (1 mM) or OMBA (1 mM). The cultures were incubated on a rotary shaker for 14 h at 28°C and centrifuged as stated above. Culture supernatant (1 ml) was transferred to a 2 ml microcentrifuge tube, acidified with 20 µl of HCl, extracted with 750 µl of EtOAc and vortexed thoroughly followed by another centrifugation step. The EtOAc phase (500 µl) was transferred to a fresh microcentrifuge tube and evaporated for 30 min in a SpeedVac (UniEquip). For IPA and Phe analysis, the samples were solved in an aqueous solution of acetonitrile (20% v/v) and trifluoroacetic acid (0.1% w/v) and subjected to HPLC (Beckman Gold) on a C18 ultrasphere column (5 µm, 4.6 × 250 mm, Beckman) eluting with 20% (v/v) acetonitrile, 0.1% trifluoroacetic acid in water for 10 min, followed by a linear gradient of 20–40% acetonitrile, 0.1% trifluoroacetic acid for 20 min at a flow rate of 1 ml min<sup>-1</sup>. Although highest peak of IPA was seen at 220 nm, absorbance was measured at 260 nm to compare amounts of IPA with amounts of Phe. IPA eluted at 25.8–26.2 min, while Phe eluted at 4.0–4.2 min. Peak areas were integrated and absorbance units were quantified as percentage of wild-type average. Three independent samples were analysed for each experiment. IPA identity was checked by comparison with standard and spiking of preparations. Phe identity was verified by MS/MS analysis after solvent evaporation from fractions containing Phe. Samples were re-dissolved in mobile phase and analysed using the same conditions as described for Met (see below). Retention time was 3.5 min. MS/MS detection was performed in positive mode using the transition 166 > 120 as quantifier, and the transition 166 > 103 as qualifier.

For analysis of Met concentration, samples were dissolved in low-pH buffer (0.1% formic acid) to ensure complete dissolution, and filtrated. Separation of a 10 µl sample was performed on a ZIC-HILIC zwitterionic column (100 × 2.1 mm, 3.5 µm, Sequant, Umeå, Sweden) under isocratic conditions with pH and temperature control [acetonitrile/ammonium acetate (20 mM, pH 6.5), 80/20; 40°C] and a flow rate of 0.1 ml min<sup>-1</sup>. Met eluted with a retention time of 4.9 min. MS/MS detection was performed in positive mode using the transition 150 > 104 as quantifier, and the transition 150 > 133 as qualifier.

### Tam1 overexpression and purification

The *tam1* ORF was amplified using primers oKZ121 (GGTACATATGACACCTTCCGCCCAAG) and oKZ122 (GGTTCTCGAGTTAAGCGAGCTCAGG) from genomic DNA of *U. maydis* wild-type strain 521. The 1.5 kb product was digested with NdeI and XhoI and inserted into the same restriction sites of the vector pET15b (Novagen, Madison, WI, USA) to yield pET15b-Tam1. Verified plasmids were transformed into the *E. coli* strain Rosetta (DE) pLysS (Novagen, Madison, WI, USA). An overnight culture (4 ml) of Rosetta (DE) pLysS pET15b-Tam1 was diluted in 300 ml YT medium containing 100 µg ml<sup>-1</sup> ampicillin and 2 µg ml<sup>-1</sup> cloramphenicol and grown at 37°C with shaking to an OD of 0.7. After the addition of 0.4 mM IPTG to the culture medium, cells were incubated at 16°C for 2.5 h, pelleted for 20 min at 4°C and stored at -80°C. Preparation of cell free extracts and Tam1 purification was according to the QIA expressionist handbook protocol 9 'Preparation of cleared *E. coli* lysates under native conditions' and protocol 12 'Batch purification of 6xHis-tagged proteins from *E. coli* under native conditions' (Qiagen, Hilden, Germany). Imidazole in the elution buffers was used at the increasing concentrations (100, 150, 200, 250 and 500 mM). A Rosetta (DE) pLysS strain containing the empty pET15b vector [Rosetta (DE) pLysS pET15b] was treated in the same way and served as a negative control. Protein concentrations were determined according to Bradford (Bradford, 1976). Protein identity was confirmed by MALDI-TOF MS/MS (Kahnt *et al.*, 2007).

### Tam1 enzyme activity assays

Reaction mixtures (200 µl) contained Tris-HCl (100 mM, pH 6.7), pyridoxal phosphate (250 µM), aminoacceptor (PPy, 2-OG or OMBA, 2 mM) and aminodonor (Trp Phe or Met, 2 mM). Tam1 enzyme was used at a concentration of 2 µM. Elution buffer 5 containing 500 mM imidazole served as mock control. Wash and elution fractions of the Rosetta (DE) pLysS pET15b strain were tested under all assay conditions specified in Fig. 5A and did not show any enzymatic activities. Reactions were carried out at 48°C for 1 h, stopped by shock freezing in liquid nitrogen and stored at -20°C.

Concentrations of Trp, IPA and Phe were determined from thawed samples by HPLC (Beckman Gold) on a C18 ultrasphere column (5 µm, 4.6 × 250 mm, Beckman) eluting with 20% (v/v) acetonitrile, 0.1% trifluoroacetic acid in water for 10 min, followed by a linear gradient of 20–40% acetonitrile, 0.1% trifluoroacetic acid for 20 min at a flow rate of 1 ml min<sup>-1</sup>. Absorbance of all three compounds was measured at 260 nm. Trp eluted at 5.1–5.3 min, IPA at 25.8–26.1 min and Phe at 4.0–4.1 min. Peak areas were integrated and absorbance units were quantified. Absorbance units of the mock control experiments (assay conditions 1–5 of Fig. 5B for Trp and assay condition 7 for Met) were set to 2 mM and served as reference. As a significant amount of IPA spontaneously degraded to IAA during the determination of IPA concentration, IPA concentration was determined by the sum of the IPA and IAA peak areas relative to standard. Analysis of Met concentration was done as described in the section *Feeding experiments*. Each assay was carried out three times.

## Acknowledgements

We thank Regine Kahmann, Dominik Begerow, Michael Bölker, Dirk Hoffmeister and Wolfgang Steglich for helpful discussions, Regine Kahmann for the gift of the genomic library of *U. maydis*, Hans-Joachim Krämer for help with initial isolation of pigments from *U. maydis*, Maria Valevich and Theresa Wollenberg for their contribution to establish pigment extraction and analysis, Kai Luh and Emine Kaya for their support in generating pphle8 and ptam2ko\_nat, Bernadette Heinze for help with feeding experiments, Kerstin Schipper for advice on purification of Tam1, Jörg Kahnt and Markus Winterberg for analytical confirmation of Tam1 purification, and Elmar Meyer for technical assistance. We acknowledge funding of Katja Zuther by the IMPRS for Environmental, Cellular and Molecular Biology. This work was supported in part by the German Science Foundation DFG via Grant SPP1160 to P.M.

## References

- Altschul, S.F., Gish, W., Miller, W., Myers, E.W., and Lipman, D.J. (1990) Basic local alignment search tool. *J Mol Biol* **215**: 403–410.
- Balibar, C.J., and Walsh, C.T. (2006) In Vitro Biosynthesis of Violacein from 1-Tryptophan by the Enzymes VioA-E from *Chromobacterium violaceum*. *Biochemistry* **45**: 15444–15457.
- Balibar, C.J., Howard-Jones, A.R., and Walsh, C.T. (2007) Terrequinone A biosynthesis through 1-tryptophan oxidation, dimerization and bisprenylation. *Nat Chem Biol* **3**: 584–592.
- Basse, C.W., Lottspeich, F., Steglich, W., and Kahmann, R. (1996) Two potential indole-3-acetaldehyde dehydrogenases in the phytopathogenic fungus *Ustilago maydis*. *Eur J Biochem* **242**: 648–656.
- Bergander, L., Wincent, E., Rannug, A., Foroosh, M., Alworth, W., and Rannug, U. (2004) Metabolic fate of the Ah receptor ligand 6-formylindolo[3,2-b]carbazole. *Chem Biol Interact* **149**: 151–164.
- Berger, L.C., Wilson, J., Wood, P., and Berger, B.J. (2001) Methionine regeneration and aspartate aminotransferase in parasitic protozoa. *J Bacteriol* **183**: 4421–4434.
- Bittinger, M.A., Nguyen, L.P., and Bradfield, C.A. (2003) Aspartate aminotransferase generates proagonists of the aryl hydrocarbon receptor. *Mol Pharmacol* **64**: 550–556.
- Bölker, M., Böhnert, H.U., Braun, K.H., Görl, J., and Kahmann, R. (1995) Tagging pathogenicity genes in *Ustilago maydis* by restriction enzyme-mediated integration (REMI). *Mol Gen Genet* **248**: 547–552.
- Brachmann, A., König, J., Julius, C., and Feldbrügge, M. (2004) A reverse genetic approach for generating gene replacement mutants in *Ustilago maydis*. *Mol Genet Genomics* **272**: 216–226.
- Bradford, M.M. (1976) A rapid and sensitive method for the quantitation of microgram quantities of protein utilizing the principle of protein-dye binding. *Anal Biochem* **72**: 248–254.
- Brenner, M., Rexhausen, H., Steffan, B., and Steglich, W. (1988) Synthesis of arcyriarubin B and related bisindolylmaleimides. *Tetrahedron* **44**: 2887–2892.
- Charles, C.R., Sire, D.J., Johnson, B.L., and Beidler, J.G. (1973) Hypopigmentation in tinea versicolor: a histochemical and electronmicroscopic study. *Int J Dermatol* **12**: 48–58.
- Fritsche, E., Schäfer, C., Calles, C., Bernsmann, T., Bernshausen, T., Wurm, M., et al. (2007) Lightening up the UV response by identification of the arylhydrocarbon receptor as a cytoplasmic target for ultraviolet B radiation. *Proc Natl Acad Sci USA* **104**: 8851–8856.
- Galadari, I., el Komy, M., Mousa, A., Hashimoto, K., and Mehregan, A.H. (1992) Tinea versicolor: histologic and ultrastructural investigation of pigmentary changes. *Int J Dermatol* **31**: 253–256.
- Garbe, T.R., Kobayashi, M., Shimizu, N., Takesue, N., Ozawa, M., and Yukawa, H. (2000) Indolyl carboxylic acids by condensation of indoles with alpha-keto acids. *J Nat Prod* **63**: 596–598.
- Gillissen, B., Bergemann, J., Sandmann, C., Schroebe, B., Bölker, M., and Kahmann, R. (1992) A two-component regulatory system for self/non-self recognition in *Ustilago maydis*. *Cell* **68**: 647–657.
- Gruen, H.E. (1959) Auxins and fungi. *Annu Rev Plant Physiol* **10**: 405–440.
- Gueho, E., Midgley, G., and Guillot, J. (1996) The genus *Malassezia* with description of four new species. *Antonie Van Leeuwenhoek* **69**: 337–355.
- Gupta, A.K., Batra, R., Bluhm, R., and Faergemann, J. (2003) Pityriasis versicolor. *Dermatol Clin* **21**: 413–429, v–vi.
- Hoffman, C.S., and Winston, F. (1987) A ten-minute DNA preparation from yeast efficiently releases autonomous plasmids for transformation of *Escherichia coli*. *Gene* **57**: 267–272.
- Holliday, R. (1974) *Ustilago Maydis*. New York: Plenum Press.
- Howard-Jones, A.R., and Walsh, C.T. (2006) Staurosporine and rebeccamycin aglycones are assembled by the oxidative action of StaP, StaC, and RebC on chromopyrrolic acid. *J Am Chem Soc* **128**: 12289–12298.
- Howard-Jones, A.R., and Walsh, C.T. (2007) Nonenzymatic oxidative steps accompanying action of the cytochrome P450 enzymes StaP and RebP in the biosynthesis of staurosporine and rebeccamycin. *J Am Chem Soc* **129**: 11016–11017.
- Iraqui, I., Vissers, S., Cartiaux, M., and Urrestarazu, A. (1998) Characterisation of *Saccharomyces cerevisiae* ARO8 and ARO9 genes encoding aromatic aminotransferases I and II reveals a new aminotransferase subfamily. *Mol Gen Genet* **257**: 238–248.
- Irlinger, B., Krämer, H.J., Mayser, P., and Steglich, W. (2004) Pityriarubins, biologically active bis (indolyl) spirans from cultures of the lipophilic yeast *Malassezia furfur*. *Angew Chem Int Ed Engl* **43**: 1098–1100.
- Irlinger, B., Bartsch, A., Krämer, H.J., Mayser, P., and Steglich, W. (2005) New tryptophan metabolites from cultures of the lipophilic yeast *Malassezia furfur*. *Helvetica Chimica Acta* **88**: 1472–1485.
- Jensen, R.A., and Gu, W. (1996) Evolutionary recruitment of biochemically specialized subdivisions of Family I within the protein superfamily of aminotransferases. *J Bacteriol* **178**: 2161–2171.
- Kahnt, J., Buchenau, B., Mahler, F., Kruger, M., Shima, S.,

- and Thauer, R.K. (2007) Post-translational modifications in the active site region of methyl-coenzyme M reductase from methanogenic and methanotrophic archaea. *Febs J* **274**: 4913–4921.
- Kämper, J. (2004) A PCR-based system for highly efficient generation of gene replacement mutants in *Ustilago maydis*. *Mol Genet Genomics* **271**: 103–110.
- Kämper, J., Kahmann, R., Bölker, M., Ma, L.J., Brefort, T., Saville, B.J., et al. (2006) Insights from the genome of the biotrophic fungal plant pathogen *Ustilago maydis*. *Nature* **444**: 97–101.
- Kaper, J.M., and Veldstra, H. (1958) On the metabolism of tryptophan by *Agrobacterium tumefaciens*. *Biochim Biophys Acta* **30**: 401–420.
- Kobayashi, K., and Yoshimoto, A. (1982) Studies on yeast sulfite reductase. IV. Structure and steady-state kinetics. *Biochim Biophys Acta* **705**: 348–356.
- Koga, J. (1995) Structure and function of indolepyruvate decarboxylase, a key enzyme in indole-3-acetic acid biosynthesis. *Biochim Biophys Acta* **1249**: 1–13.
- Kradolfer, P., Niederberger, P., and Hutter, R. (1982) Tryptophan degradation in *Saccharomyces cerevisiae*: characterization of two aromatic aminotransferases. *Arch Microbiol* **133**: 242–248.
- Krämer, H.J., Podobinska, M., Bartsch, A., Battmann, A., Thoma, W., Bernd, A., et al. (2005a) Malassezin, a novel agonist of the aryl hydrocarbon receptor from the yeast *Malassezia furfur*, induces apoptosis in primary human melanocytes. *Chembiochem* **6**: 860–865.
- Krämer, H.J., Kessler, D., Hipler, U.C., Irlinger, B., Hort, W., Bödeker, R.H., et al. (2005b) Pityriarubins, novel highly selective inhibitors of respiratory burst from cultures of the yeast *Malassezia furfur*: comparison with the bisindolylmaleimide arcyriarubin A. *Chembiochem* **6**: 2290–2297.
- Larangeira de Almeida, H., Jr and Mayser, P. (2006) Absence of sunburn in lesions of pityriasis versicolor alba. *Mycoses* **49**: 516.
- Larkin, M.A., Blackshields, G., Brown, N.P., Chenna, R., McGettigan, P.A., McWilliam, H., et al. (2007) Clustal W and Clustal X version 2.0. *Bioinformatics* **23**: 2947–2948.
- Ljung, K., Hull, A.K., Kowalczyk, M., Marchant, A., Celenza, J., Cohen, J.D., and Sandberg, G. (2002) Biosynthesis, conjugation, catabolism and homeostasis of indole-3-acetic acid in *Arabidopsis thaliana*. *Plant Mol Biol* **49**: 249–272.
- Machowinski, A., Krämer, H.J., Hort, W., and Mayser, P. (2006) Pityriacitrin – a potent UV filter produced by *Malassezia furfur* and its effect on human skin microflora. *Mycoses* **49**: 388–392.
- Mayser, P., Wille, G., Imkamp, A., Thoma, W., Arnold, N., and Monsees, T. (1998) Synthesis of fluorochromes and pigments in *Malassezia furfur* by use of tryptophan as the single nitrogen source. *Mycoses* **41**: 265–271.
- Mayser, P., Schäfer, U., Krämer, H.J., Irlinger, B., and Steglich, W. (2002) Pityriacitrin – an ultraviolet-absorbing indole alkaloid from the yeast *Malassezia furfur*. *Arch Dermatol Res* **294**: 131–134.
- Mayser, P., Stapelkamp, H., Krämer, H.J., Podobinska, M., Wallbott, W., Irlinger, B., and Steglich, W. (2003) Pityrialactone- a new fluorochrome from the tryptophan metabolism of *Malassezia furfur*. *Antonie Van Leeuwenhoek* **84**: 185–191.
- Mayser, P., Wenzel, M., Krämer, H.J., Kindler, B.L., Spittler, P., and Haase, G. (2007) Production of indole pigments by *Candida glabrata*. *Med Mycol* **45**: 519–524.
- Nebert, D.W., and Dalton, T.P. (2006) The role of cytochrome P450 enzymes in endogenous signalling pathways and environmental carcinogenesis. *Nat Rev Cancer* **6**: 947–960.
- Nishizawa, T., Gruschow, S., Jayamaha, D.H., Nishizawa-Harada, C., and Sherman, D.H. (2006) Enzymatic assembly of the bis-indole core of rebeccamycin. *J Am Chem Soc* **128**: 724–725.
- Oberg, M., Bergander, L., Hakansson, H., Rannug, U., and Rannug, A. (2005) Identification of the tryptophan photoproduct 6-formylindolo[3,2-b]carbazole, in cell culture medium, as a factor that controls the background aryl hydrocarbon receptor activity. *Toxicol Sci* **85**: 935–943.
- Okey, A.B., Riddick, D.S., and Harper, P.A. (1994) Molecular biology of the aromatic hydrocarbon (dioxin) receptor. *Trends Pharmacol Sci* **15**: 226–232.
- Oxford, G.S., and Gillespie, R.G. (1998) Evolution and ecology of spider coloration. *Annu Rev Entomol* **43**: 619–643.
- Paris, C.G., and Magasanik, B. (1981) Purification and properties of aromatic amino acid aminotransferase from *Klebsiella aerogenes*. *J Bacteriol* **145**: 266–271.
- Pedras, M.S., Okanga, F.I., Zaharia, I.L., and Khan, A.Q. (2000) Phytoalexins from crucifers: synthesis, biosynthesis, and biotransformation. *Phytochemistry* **53**: 161–176.
- Politi, V., De Luca, G., Di Stazio, G., Materazzi, M., inventors. Cosmetic use of 3-indolepyruvic acid. *US Patent 5091172*. Issue date: February 25, 1992.
- Rannug, U., Rannug, A., Sjöberg, U., Li, H., Westerholm, R., and Bergman, J. (1995) Structure elucidation of two tryptophan-derived, high affinity Ah receptor ligands. *Chem Biol* **2**: 841–845.
- Reineke, R., Heinze, B., Buettner, H., Schirawski, J., Kahmann, R., and Basse, C.W. (2008) Indole-3-acetic acid biosynthesis in the smut fungus *Ustilago maydis* and its relevance for increased IAA levels in infected tissue and host tumour formation. *Mol Plant Pathol* (in press).
- Russell, G.A., and Kaupp, G. (1969) Oxidation of carbanions. IV. Oxidation of indoxyl to indigo in basic solutions. *J Am Chem Soc* **91**: 3851–3859.
- Sambrook, J., Fritsch, E.F., and Maniatis, T. (1989) *Molecular Cloning, a Laboratory Manual*, 2nd edn. Cold Spring Harbor NY: Cold Spring Harbor Laboratory Press.
- Sanchez, C., Mendez, C., and Salas, J.A. (2006) Indolocarbazole natural products: occurrence, biosynthesis, and biological activity. *Nat Prod Rep* **23**: 1007–1045.
- Schneider, P., Weber, M., Rosenberger, K., and Hoffmeister, D. (2007) A one-pot chemoenzymatic synthesis for the universal precursor of antidiabetes and antiviral bisindolylquinones. *Chem Biol* **14**: 635–644.
- Schulz, B., Banuett, F., Dahl, M., Schlesinger, R., Schäfer, W., Martin, T., et al. (1990) The *b* alleles of *U. maydis*, whose combinations program pathogenic development code for polypeptides containing a homeodomain-related motif. *Cell* **60**: 295–306.
- Spaepen, S., Vanderleyden, J., and Remans, R. (2007) Indole-3-acetic acid in microbial and microorganism-plant signaling. *FEMS Microbiol Rev* **31**: 425–448.

- Sung, M.H., Tanizawa, K., Tanaka, H., Kuramitsu, S., Kagamiyama, H., Hirotsu, K., *et al.* (1991) Thermostable aspartate aminotransferase from a thermophilic *Bacillus* species. Gene cloning, sequence determination, and preliminary x-ray characterization. *J Biol Chem* **266**: 2567–2572.
- Teale, W.D., Paponov, I.A., and Palme, K. (2006) Auxin in action: signalling, transport and the control of plant growth and development. *Nat Rev Mol Cell Biol* **7**: 847–859.
- Thoma, W., Krämer, H.J., and Mayser, P. (2005) Pityriasis versicolor alba. *J Eur Acad Dermatol Venereol* **19**: 147–152.
- Tsai, H.F., Wang, H., Gebler, J.C., Poulter, C.D., and Schardl, C.L. (1995) The *Claviceps purpurea* gene encoding dimethylallyltryptophan synthase, the committed step for ergot alkaloid biosynthesis. *Biochem Biophys Res Commun* **216**: 119–125.
- Tudzynski, P., Hölter, K., Correia, T., Arntz, C., Grammel, N., and Keller, U. (1999) Evidence for an ergot alkaloid gene cluster in *Claviceps purpurea*. *Mol General Genet* **261**: 133–141.
- Tudzynski, P., Correia, T., and Keller, U. (2001) Biotechnology and genetics of ergot alkaloids. *Appl Microbiol Biotechnol* **57**: 593–605.
- Urrestarazu, A., Vissers, S., Iraqui, I., and Grenson, M. (1998) Phenylalanine- and tyrosine-auxotrophic mutants of *Saccharomyces cerevisiae* impaired in transamination. *Mol Gen Genet* **257**: 230–237.
- Vlassis, A.A., Bartos, D., and Trunkey, D. (1990) Importance of spontaneous alpha-ketoacid decarboxylation in experiments involving peroxide. *Biochem Biophys Res Commun* **170**: 1281–1287.
- Vogler, H., and Kuhlemeier, C. (2003) Simple hormones but complex signalling. *Curr Opin Plant Biol* **6**: 51–56.
- Wei, Y.D., Helleberg, H., Rannug, U., and Rannug, A. (1998) Rapid and transient induction of CYP1A1 gene expression in human cells by the tryptophan photoproduct 6-formylindolo[3,2-b]carbazole. *Chem Biol Interact* **110**: 39–55.
- Wille, G., Mayser, P., Thoma, W., Monsees, T., Baumgart, A., Schmitz, H.J., *et al.* (2001) Malassezin – A novel agonist of the arylhydrocarbon receptor from the yeast *Malassezia furfur*. *Bioorg Med Chem* **9**: 955–960.
- Wolf, F. (1952) The production of indole acetic acid by *Ustilago zaeae*, and its possible significance in tumor formation. *Proc Natl Acad Sci USA* **38**: 106–111.
- Woodward, A.W., and Bartel, B. (2005) Auxin: regulation, action, and interaction. *Ann Bot (Lond)* **95**: 707–735.